Article

Biosynthesis and Multifaceted Characterization of *Breynia nivosa*-Derived Silver Nanoparticles: An Eco-Friendly Approach for Biomedical Applications

Kanwal Irshad, Muhammad Sajid Hamid Akash,* Kanwal Rehman,* Ahmed Nadeem, and Asif Shahzad

Read Online

ACCESS | Metrics & More | Article Recommendations

ABSTRACT: This study presents an environmentally friendly synthesis of stable silver nanoparticles (Ag-NPs) using the methanolic extract of *Breynia nivosa*. Initial phytochemical analysis of the extract revealed the presence of alkaloids, flavonoids, glycosides, saponins, and tannins. Further characterization through high-performance liquid chromatography (HPLC) and gas chromatography−mass spectrometry (GC-MS) analyses identified a diverse array of bioactive compounds, including hydroquinone, stearic acid, neophytadiene, 9,12-octadecadienoic acid (Z,Z), methyl ester, and others. The addition of *B. nivosa* methanolic extract to an $AgNO_3$ solution resulted in a color change, confirming the green synthesis of Ag-NPs through the reduction of $AgNO_3$, as made evident by ultraviolet−visible (UV−vis) spectroscopy. X-ray diffraction (XRD) analysis provided valuable insights into the crystal structure, and scanning electron microscopy (SEM) analysis visualized the predominantly spherical shape of the Ag-NPs. However, the zeta (ζ)-potential and dynamic light scattering (DLS) analyses confirmed the stability and nanoscale dimensions of the synthesized Ag-NPs. Meanwhile, Fourier transform infrared (FT-IR) spectra exhibited peaks indicative of various functional groups, including carboxylic acids, phenols, alkanes, and isocyanates. These functional groups played a crucial role in both the reduction and capping processes of the Ag-NPs. The study further explored the antioxidant activity, cytotoxicity, acetylcholinesterase inhibition, and α-amylase inhibition activities of the Ag-NPs of the *B. nivosa* extract, demonstrating their potential for biomedical and therapeutic applications. In conclusion, this environmentally sustainable synthesis of Ag-NPs from the *B. nivosa* extract, enriched with bioactive secondary metabolites detected through HPLC and GC-MS analysis, holds promise for diverse applications in the burgeoning field of green nanotechnology.
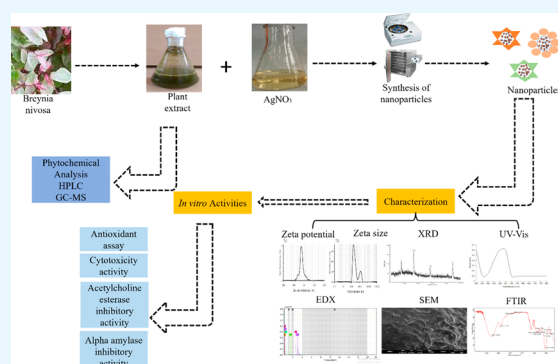
INTRODUCTION

Nanotechnology has a broad range of applications in medicine, food, agriculture, and the environment.[1] One of its main focuses is the biological synthesis of nanoparticles, achieved through physical, chemical, or biological processes to improve the quality of medicine for human health and disease conditions.[2] Among these methods, the biological approach is the most economical, environmentally friendly, and preferable over physical and chemical methods. It involves the use of medicinal plants or microorganisms for nanoparticle synthesis.[3] Green synthesis is a specific biological method that utilizes medicinal plants for nanoparticle preparation.[4] The incorporation of medicinal plants in nanotechnology offers advantages due to the presence of phytochemicals in medicinal plants, which exhibit many pharmacological activities and enhance the properties of nanoparticles.[1,5] Nanoparticles synthesized through green synthesis show promise as innovative agents for various biological activities, including antiviral, antibacterial, and antioxidant effects, without causing serious side effects.[6] In the green synthesis method, the

phytochemicals present in the plant extracts act as strong capping agents and stabilizers, preventing the aggregation or coagulation of nanoparticles.[7] Researchers have reported the successful synthesis of silver nanoparticles (Ag-NPs) using different morphological parts of plants, such as leaves stems, seeds, and flowers.[8] Phytochemicals in the plant extracts play a vital role in reducing silver ions to form Ag-NPs.[9] Each plant extract has a unique composition of phytochemicals, contributing to their distinctive characteristics.[10] The technological parameters and physiochemical characteristics of nanoparticles are particularly their size, stability, and morphology that depend upon the method of extract

preparation, solvent nature, temperature, and pH of the reaction mixture.[11]

Breynia nivosa belongs to the family *Phyllanthaceae* and is commonly known as snow brush.[12] It is a tropical shrub known for its attractive foliage, reaching a height of about 2 m, and is commonly found in public places and gardens. The plant has small mottled and variegated leaves in green, white, and red colors.[13] *B. nivosa* is traditionally used for treating toothache, tooth infections, and headaches.[14] In southeastern Nigeria, the stem of *B. nivosa* is used as a chewing stick and its leaves have been found to possess antimicrobial activity[15] as well as antioxidant, anti-inflammatory, and analgesic properties.[14] The plant's active constituents and/or secondary metabolites have significant pharmacological and biological importance[16] and are often part of the human diet. Many of these active constituents contribute to reducing the risk of diseases through their antioxidant activities. Oxidative stress occurs when there is an overproduction of reactive oxygen species (ROS) that can interact with various biomolecules such as lipid membranes, DNA, and proteins, leading to the development of different diseases including cancer, diabetes mellitus,[17] cardiovascular disease,[18] and Alzheimer's disease.[19] Green-synthesized nanoparticles have been reported in the literature to possess strong antioxidant potential, thanks to the presence of phytochemicals on their surface, which act as free radical scavengers.[20]

In this study, Ag-NPs were synthesized using the green synthesis method from the methanolic extract of *B. nivosa*. While previous studies have evaluated the production of Ag-NPs using various plant extracts for pharmacological evaluation, this research is the first report on Ag-NPs synthesized from *B. nivosa* extract. The study involves the preparation of the plant extract and a qualitative analysis of phytochemicals, and to characterize the synthesized Ag-NPs, we employed various techniques, including ultraviolet−visible (UV−vis) spectroscopy, Fourier transform infrared (FT-IR) spectroscopy, X-ray diffraction analysis (XRD), energy-dispersive X-ray (EDX), zeta (ζ)-potential, dynamic light scattering (DSL), and scanning electron microscopy (SEM). The primary objective of the study was to perform the green synthesis and characterize the morphology, size, structure, and composition of the Ag-NPs derived from *B. nivosa* extract. Additionally, the experiment was designed to investigate the *in vitro* analysis of the pharmacological potential of synthesized Ag-NPs of *B. nivosa* extract.

■ MATERIALS AND METHODS

Chemicals and Reagents. All of the reagents and chemicals used in the experiments were of high-quality analytical grade. Silver nitrate (AgNO$_3$), 1,1-diphenyl-2-picrylhydrazyl (DPPH), ascorbic acid, potassium iodide, iodine, ferric chloride, glacial acetic acid, and sulfuric acid were purchased from Sigma-Aldrich. For the experiments, freshly prepared deionized and distilled water was used.

Collection and Drying of *B. nivosa*. The leaves of the *B. nivosa* plant were collected from Faisalabad Nursery in September 2022. The plant was identified and authenticated by an expert botanist, Dr. Mansoor Hameed, from the Department of Botany, University of Agriculture Faisalabad (UAF) Pakistan, and assigned a voucher number "99−1−2022" to this plant and deposited in the herbarium of UAF.

Preparation of Methanolic Extract of *B. nivosa*. The leaves were allowed to dry at room temperature for 14 days. After drying, the leaves of *B. nivosa* were ground to form a coarse powder using a grinder. The resulting coarse powder, weighing 500 g, was then macerated in 800 mL of methanol for a period of 2 days with occasional shaking at room temperature. After 48 h, the macerate was decanted and filtered using Whatman filter paper. Following the first filtration, the obtained mixture was soaked again in 400 mL of methanol for another 48 h. Afterward, the mixture was once again decanted and filtered with a Whatman filter paper. The resulting mixture was further soaked in 200 mL of methanol for an additional 48 h. After this period, the sample was decanted and filtered again. To concentrate the extract, it was subjected to a rotary evaporator under pressure at 30 °C.

Screening of Phytochemicals. The methanolic extract of *B. nivosa* was screened for the presence of alkaloids, flavonoids, tannins, glycosides, and saponins. The qualitative results indicating the presence of phytochemicals are represented as (+) for the presence and (−) absence of phytochemicals. The presence of alkaloids in the extract of *B. nivosa* was confirmed using the Wagner's test.[21] The alkaline reagent test confirmed the presence of flavonoids.[22] To determine the presence of glycosides, the Keller−Killiani test was employed.[23] The presence of saponins and tannins was confirmed by following the procedures described in the literature.[24]

HPLC Analysis of Methanolic Extract of *B. nivosa*. HPLC analysis was conducted to detect the phenolic compounds in the methanolic extract of *B. nivosa*. The analysis was carried out using an HPLC system (PerkinElmer) equipped with a Flexar binary liquid chromatography pump and a C-18 column with an internal diameter of 4.6 mm and a particle size of 5 μm, connected to a UV−vis detector that was controlled by software. The mobile phase consisted of two solvents, denoted as solvents A and B. Solvent A was a mixture of methanol and acetonitrile in a ratio of 30:70, while Solvent B was a mixture of 0.5% glacial acetic acid and double-distilled water. UV spectra at 275 nm were obtained to analyze the results. The retention times of all peaks were compared with the retention times of standards. HPLC is an efficient method for identifying compounds based on their retention times.[25]

GC-MS Analysis of Methanolic Extract of *B. nivosa*. GC-MS analysis was conducted to identify the compounds present in the methanolic extract of *B. nivosa*. Sample derivatization was carried out using the trimethylsilyl derivatization method. Initially, 20 μL of the sample was allowed to evaporate in an oven at 80 °C for 25 min. Subsequently, the dried sample was dissolved in an 80 μL solution of methoxyamine hydrochloride in pyridine (2 mg/100 mL). The mixture was thoroughly mixed using a vortex and incubated at 30 °C for 30 min before analysis.[26] GC-MS analysis of the methanolic extract of *B. nivosa* was performed using Agilent Technologies equipment, specifically the Model No: 7890B GC system and Agilent 5977B GC/MSD. Helium gas was employed as the carrier gas at a flow rate of 1 mL/min. The injector temperature was maintained at 270 °C. The oven temperature profile was designed to gradually increase from 70 to 200 °C (with a 10 °C rise in temperature every minute), followed by a hold at 310 °C for 5 min, with an additional 10 °C increase every minute. MS was operated in electron ionization mode at 70 eV, using an electron multiplier voltage of 1859 V. The retention times of the detected compounds were determined by using Chemstation software. The confirmation of various phytochemicals was established by comparing their spectral data with those of authenticated

compounds in the National Institute of Standards and Technology (NIST) library.

Preparation of Silver Nanoparticles. A 1 M aqueous solution of $AgNO_3$ was prepared by dissolving 16.9 g of $AgNO_3$ in 100 mL of deionized water. Approximately 50 mL of *B. nivosa* extract was mixed with the $AgNO_3$ solution while continuously stirring at 90 °C until the mixture changed from yellow to reddish-brown. The extract of *B. nivosa* served as a capping agent in the synthesis process. The solution was then subjected to centrifugation at 4000 rpm for 60 min, causing the synthesized nanoparticles to settle at the bottom of the centrifuge tubes. The settled nanoparticles were redispersed by shaking and subsequently subjected to hot air drying at 100 °C for 60 min. Finally, the sample was stored for further characterization of the Ag-NPs.

Characterization of Nanoparticles. *UV−Vis Analysis.* UV−vis spectrum was obtained using a UV−vis spectroscopy instrument (PerkinElmer UV). A 0.5 mL suspension of Ag-NPs from *B. nivosa* was analyzed at room temperature. The reaction progress was determined by monitoring the reaction between silver ions and the *B. nivosa* extract over a wavelength range of 200−800 nm.[27]

FT-IR Analysis. The functional groups in phytochemicals involved in the process of degradation were categorized by using FT-IR Spectroscopy (Bruker α-P FT-IR). To obtain FT-IR spectra, the solution of prepared Ag-NPs was centrifuged at 10,000 rpm for half an hour. The resulting pellets were washed three times with distilled water to remove free proteins and enzymes that are not responsible for capping the Ag-NPs. Afterward, the pellets were allowed to dry by using a vacuum drier and analyzed by FT-IR.

X-ray Diffraction Analysis. The structure of the fabricated Ag-NPs was analyzed by using XRD (XRD-6000; Shimadzu). A thin layer of the synthesized Ag-NPs was prepared by immersing a glass plate in Ag-NPs solution and subjecting it to XRD analysis. The average size of the synthesized Ag-NPs was estimated using the Debye−Scherrer equation.[28]

Scanning Electron Microscopy Analysis. To observe the morphology of the synthesized Ag-NPs, a pellet was analyzed using SEM (WebFX). A very small amount of Ag-NPs was placed on a copper grid coated with carbon to form a thin film. The excess sample was removed using blotting paper, and the sample was dried before analysis.[29]

Energy-Dispersive X-ray Analysis. Energy-dispersive X-ray spectroscopy (EDX) is employed to determine the elemental composition of samples, particularly those with thin films. EDX not only provides information about the relative number of atoms but also allows for the mapping of their distribution. In this study, EDX analysis was conducted on stable synthesized Ag-NPs. For EDX analysis, the sample was prepared on a copper grid coated with carbon (model). EDX spectroscopy leverages the wave-particle duality of light and the photon nature of X-rays, providing valuable results. The EDX procedure involved measuring the intensity distribution and energy of X-rays generated by a precisely focused electron beam on the sample, which was operated at 120 keV.[30]

ζ-Potential and Dynamic Light Scattering Analysis. ζ-potential and DLS tests were used to determine the size of Ag-NPs, the homogeneity of distribution, and the charge on synthesized Ag-NPs. The measurements were conducted by using a particle analyzer (Anton Paar) for ζ-potential and a Litesizer 500 for DLS analysis. Before the measurements, the sample of synthesized nanoparticles was prepared by diluting it

with analytical grade methanol and then allowed to sonicate for 15 min.[31]

***In Vitro* Analysis of Pharmacological Activities of Ag-NPs of *B. nivosa* Extract.** *Analysis of Antioxidant Activity.* To evaluate the antioxidant activity of the synthesized Ag-NPs from *B. nivosa* extract, a DPPH free radical scavenging activity assay was performed. In the DPPH assay, DPPH is a stable free radical with a deep purple color. When antioxidants are present in the sample, they can donate hydrogen atoms to the DPPH radical, leading to its reduction. As a result, the color of the DPPH radical changes from purple to yellow, indicating the scavenging of the free radical by the antioxidant compounds. The antioxidant potential of the synthesized Ag-NPs was determined at various concentrations (e.g., 25, 50, 75, and 100 μg/mL). The reaction mixture containing the Ag-NPs and DPPH was incubated in the dark for a specific period, allowing sufficient time for the scavenging reaction to occur. The decrease in absorbance at a specific wavelength was measured using a spectrophotometer, and the percentage of DPPH scavenging was calculated based on the change in absorbance. Ascorbic acid, which is a known antioxidant, was used as a positive control in the assay. The DPPH assay provided valuable information about the ability of the synthesized Ag-NPs to act as free radical scavengers, thus assessing their potential antioxidant activity.

The free radical scavenging capability of *B. nivosa* extract and the fabricated Ag-NPs of *B. nivosa* was evaluated using the DPPH assay, following the procedure as described in the literature with slight modifications.[32] The antioxidant activity of both the *B. nivosa* extract and the Ag-NPs was estimated by determining their hydrogen atom donating capacity, which leads to the decolorization of a methanolic solution of DPPH. The reaction mixture was uniformly stirred and then placed in the dark for 30 min at room temperature. The absorbance of the reaction mixture was measured at 517 nm using a spectrophotometer. Ascorbic acid was used as the standard antioxidant in this experiment.[33] The percentage of free radical scavenging was calculated using the following equation:

$$\% \text{ of free radical scavenging} = \frac{A_0 - A_1}{A_0} \times 100 \tag{1}$$

where A_0 and A_1 represent the absorbances of the control and the sample, respectively. The percentage of inhibition was calculated using the formula

$$\text{percentage of inhibition} = (1 - A_0 A_1) \times 100 \tag{2}$$

The percentage of inhibition was then plotted against the different concentrations of the *B. nivosa* extract and synthesized Ag-NPs. The entire experiment was repeated three times for each concentration to ensure reliability and accuracy. The IC_{50} value, which represents the concentration required to inhibit 50% of the DPPH radicals, was calculated from the percentage of inhibition plotted against the different concentrations of the extract at 515 nm. By determination of the IC_{50} value, the antioxidant potential of both the methanolic extract of *B. nivosa* and the synthesized Ag-NPs can be quantified, allowing for a comparison of their scavenging abilities against the DPPH radicals.

Analysis of Cytotoxic Activity. Cell Culture. MCF7 human breast cancer cells were cultured in Dulbecco's modified Eagle's medium (DMEM) supplemented with 10% fetal bovine serum (FBS), 100 μg/mL of streptomycin, and 100

units/mL of penicillin. The cells were maintained at 37 °C in a 5% CO_2 atmosphere with moderate humidity. Subsequently, the cells were treated with a methanolic extract of *B. nivosa* and Ag-NPs prepared from *B. nivosa* extract. The nanoparticles were dissolved in DMSO to achieve a final concentration of 0.05%.[34]

Cell Viability Assay. Cell viability was assessed using 3-(4,5-dimethylthiazol-2-yl)-2,5-diphenyl-2*H*-tetrazolium bromide (MTT), following a previously described method.[35] MCF7 breast cancer cells were treated with *B. nivosa* extract and prepared Ag-NPs at concentrations of 200, 400, and 600 for 48 h. After the incubation period, 10 μL of MTT reagent was added, and the cells were further incubated for 4 h at 37 °C. Subsequently, 150 μL of DMSO was added to dissolve the formazan crystals, and the absorbance of the sample was measured at 490 nm. The percentage of cell viability was then calculated using the following formula:

$$\text{cell viability (\%)} = \frac{\text{absorbance by sample}}{\text{absorbance by control}} \times 100 \tag{3}$$

Analysis of Acetylcholinesterase Inhibition Activity. The acetylcholine inhibition activity of *B. nivosa* extract and the synthesized Ag-NPs was determined using protocols with slight modifications as previously described.[36] In this assay, acetylcholine iodide served as the substrate reagent and 5,5′-dithio-bis(2-nitrobenzoic) acid (DTNB) was utilized to evaluate the activity of acetylcholinesterase. Eserine was employed as a reference compound. The reaction mixture consisted of cholinesterase enzyme (10 μL), a sample at a concentration of 0.5 mg/mL, 0.05 mM phosphate buffer (60 μL, pH 7.7), and 0.05 mM DTNB (10 μL). This mixture was allowed to incubate for 30 min at 37 °C. The change in optical density (OD) was then measured following the addition of acetylcholine iodide (10 μL) at 405 nm. The percentage inhibition of the sample was calculated using the formula below

$$\text{percentage inhibition} = \frac{\text{Abs}(S) - \text{Abs}(T)}{\text{Abs}(S)} \times 100 \tag{4}$$

where Abs (S) is the absorbance of standard and Abs(T) is the absorbance of test sample. IC_{50} was calculated from the graph plotted between percentage of inhibition and concentrations.

Analysis of α-Amylase Inhibition Activity. The *B. nivosa* extract and synthesized Ag-NPs were mixed with 0.5 mg/mL starch (2% w/v) and 1 U/mL of a human pancreatic α-amylase solution (250 μL) in a test tube to achieve homogeneity. The solution was then incubated at 20 °C for 3−5 min. After incubation, a colored reagent (dinitrosalicylic acid) was added to each well to halt the enzymatic reaction. The mixture was then heated in boiling water, and an additional 250 μL of α-amylase solution was introduced. The mixture was continuously heated for 15 min and then allowed to cool to room temperature. Distilled water was added to the mixture to reach a total volume of 6000 μL and mixed thoroughly using a vortex mixer. The potential of *B. nivosa* extract and Ag-NPs to inhibit α-amylase was determined by measuring the absorbance at 540 nm using a double-beam UV−vis spectrophotometer (TU 1901 plus), with acarbose as the standard, as reported previously.[37] The percentage inhibition was calculated using the formula below

$$\text{percentage inhibition} = \frac{\text{Abs}(S) - \text{Abs}(T)}{\text{Abs}(S)} \times 100 \tag{5}$$

where Abs (S) is the absorbance of standard and Abs (T) is the absorbance of test sample. IC_{50} was calculated from the graph plotted between percentage of inhibition and concentrations.

Statistical Analysis. The results of the *in vitro* experiments are expressed as mean ± standard deviation (SD) using GraphPad Prism version 5. Statistical analysis was performed using one-way ANOVA followed by Tukey's multiple comparison test. $P > 0.05$ was considered statistically significant.

■ RESULTS

Phytochemicals Analysis. The phytochemical analysis results of the *B. nivosa* extract are presented in Table 1. The

Table 1. Result of Phytochemical Analysis of the *B. nivosa* Extract

phytochemicals	result
alkaloids	+
flavonoids	+
glycosides	+
saponins	+
tannins	+

constituents of the phytochemicals responsible for reducing and capping the fabricated Ag-NPs were analyzed quantitatively. It was concluded that the *B. nivosa* extract contains alkaloids, flavonoids, glycosides, tannins, and saponins, making it a rich source of phytochemicals. Our results are consistent with the reported findings in the literature.[38]

HPLC Analysis of *B. nivosa* Extract. HPLC is an analytical technique for the separation of individual components in plant extract. HPLC has potential for fingerprinting, quantification, and authentication of herbal products. The chromatogram of methanolic extract of *B. nivosa* is shown in Figure 1 along with chromatogram of standards compounds. The phytochemicals were identified in HPLC hydroxybenzoic acid, p-coumaric acid, and vanillic acid (Figure 1 and Table 2).

GC-MS Analysis of *B. nivosa* Extract. A total of 26 compounds were identified through GC-MS analysis of the methanolic extract of *B. nivosa* (Figure 2). These 26 peaks corresponded to various bioactive compounds; their identification was confirmed by assessing retention time, peak height, peak area, and fragmentation patterns against the NIST library. The identified compounds contribute to the phytochemical and biological activities. Details of these identified compounds, including their retention times, molecular weights, and percentage concentrations, are presented in Table 3. The mass spectra of these identified compounds in the methanolic extract of *B. nivosa* are displayed in Figure 3. The chemical structures were predicted from the mass spectra based on the fragmentation patterns of each identified compound. The fragmentation pattern generated various peaks, depending on their mass-to-charge ratio (m/z).

Characterization of Ag-NPs of *B. nivosa* Extract. *UV−Vis Spectroscopy.* UV−vis spectroscopy was employed for the optical characterization of the synthesized Ag-NPs. The reduction of silver ions (Ag^+ to Ag^0) was achieved using the *B. nivosa* methanolic extract, and the reaction was continuously
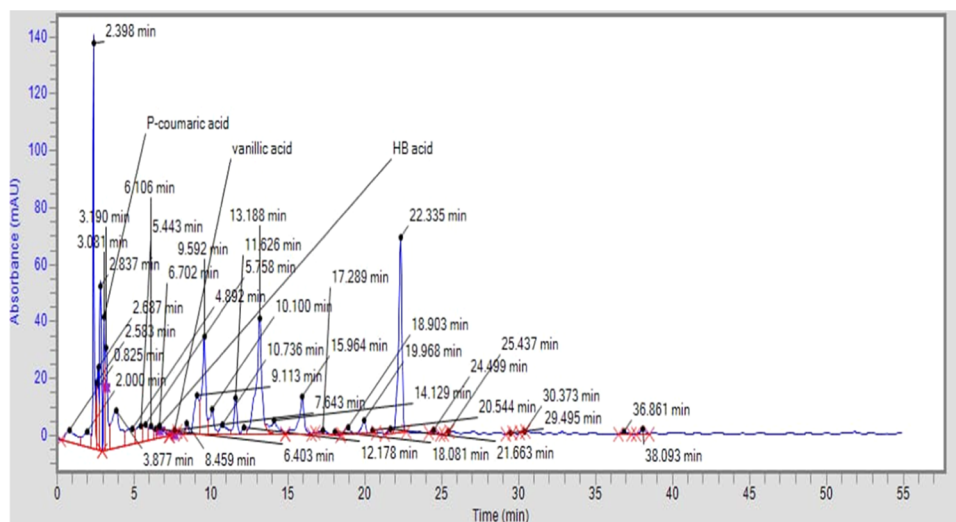
Figure 1. Chromatogram of methanolic extract of *B. nivosa*.

Table 2. Identified Compounds from a Methanolic Extract of *B. nivosa*

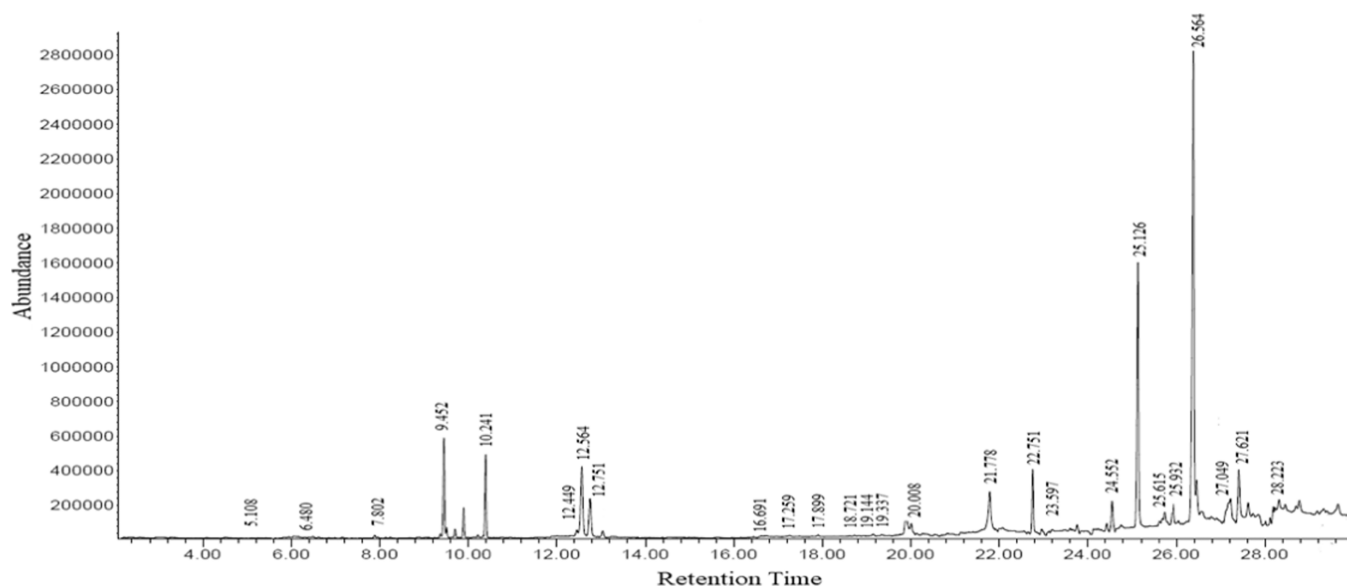| Phytochemicals	Retention time (min)	Area	Height	Structures
p-coumaric acid	3.081	293,889.3	47,470.7	
Hydroxybenzoic acid	6.702	110,297.4	3,925.6	
Vanillic acid	7.643	13,715.1	910.8	

Figure 2. GC-MS spectrum of a methanolic extract of *B. nivosa*.

monitored using a UV−vis spectrophotometer to verify its efficacy and suitability for nanoparticle synthesis. Initially, the

synthesis of Ag-NPs was observed when the color of the reaction mixture changed from yellow to brown, indicating the

Table 3. Bioactive Compounds Identified from GC-MS Analysis of the Methanolic Extract of *B. nivosa*

sr.#	compounds	retention time	concentration (%)	molecular weight	molecular formula
1	hydroquinone	5.108	90	110.11 g/mol	$C_6H_6O_2$
2	stearic acid	6.480	60	284.48 g/mol	$CH_3(CH_2)_{16}CO_2H$
3	9,12-octadecadienoic acid (Z,Z)-, methyl ester	7.802	87	294.47 g/mol	$C_{19}H_{34}O_2$
4	neophytadiene	9.452	96	278.51 g/mol	$C_{20}H_{38}$
5	curan-17-oic acid, 2,16-didehydro-19,20-dihydroxy-, methyl ester	10.241	83	356.4 g/mol	$C_{20}H_{24}N_2O_4$
6	methyl 9-*cis*,11-*trans*-octadecadienoate	12.449	97	294.47 g/mol	$C_{19}H_{34}O_2$
7	9,12,15-octadecatrienoic acid, methyl ester, (Z,Z,Z)-	12.564	99	292.45 g/mol	$C_{19}H_{32}O_2$
8	phytol	12.751	97	296.53 g/mol	$C_{20}H_{40}O$
9	7,10,13-hexadecatrienoic acid, methyl ester	16.691	90	264.4 g/mol	$C_{17}H_{28}O_2$
10	cyclopropaneoctanoic acid, 2-[[2-[(2-ethylcyclopropyl)methyl]cyclopropyl]methyl]-, methyl ester	17.259	90	334.5 g/mol	$C_{22}H_{38}O_2$
11	2,6,10-dodecatrien-1-ol, 3,7,11-trimethyl-	17.899	65	222.36 g/mol	$C_{15}H2_6O$
12	methyl 8,11,14-heptadecatrienoate	18.721	96	13278.4 g/mol	$C_{18}H_{30}O_2$
13	15,24-dimethyl-1,4,7,10,18,21-hexaoxa-15,24-diazacyclooctacosane-11,14,25,28-tetrone	19.144	89	412.7 g/mol	$C_{29}H_{48}O$
14	(7R,8R)-*cis*-anticis-tricyclo[7.3.0.0(2,6)]dodecane-7,8-diol	19.337	90	196.29 g/mol	$C_{12}H_{20}O_2$
15	phthalic acid, monooctyl ester	20.008	80	278.34 g/mol	$C_{16}H_{22}O_4$
16	8,11,14-eicosatrienoic acid, methyl ester, (Z,Z,Z)-	21.778	89	320.5	$C_{21}H_{36}O_2$
17	supraene	22.751	90	410.71 g/mol	$C_{30}H_{50}$
18	*trans*-geranylgeraniol	23.579	65	290.48 g/mol	$C_{20}H_{34}O$
19	γ.-tocopherol	24.552	96	416.7 g/mol	$C_{28}H_{48}O_2$
20	dl-α-tocopherol	25.126	99	430.7 g/mol	$C_{29}H_{50}O_2$
21	ergosta-5,7-dien-3-ol, (3β)-	25.615	89	398.7 g/mol	$C_{28}H_{46}O$
22	stigmasterol	25.932	92	412.7 g/mol	$C_{29}H_{48}O$
23	pyridine-3-carboxamide, oxime, N-(2-trifluoromethylphenyl)-	26.564	95	281.23 g/mol	$C_{13}H_{10}F_3N_3O$
24	squalene	27.049	89	410.7 g/mol	$C_{30}H_{50}$
25	lanosterol	27.621	73	426.7 g/mol	$C_{30}H_{50}O$
26	geranylgeraniol	28.223	63	290.5 g/mol	$C_{20}H_{34}O$

reduction of $AgNO_3$ to Ag-NPs. The optical absorbance of the sample mixture was then recorded over the wavelength range of 200−800 nm (Figure 4). A strong absorption peak was observed between 400 and 438 nm in the visible region, which was attributed to the phenomenon of surface plasmon resonance (SPR) of the fabricated Ag-NPs. The absorption peak of SPR occurs due to the oscillation of free electrons in the conduction band of metals resonating with light simultaneously.[39] The position of the absorption band is influenced by the size of the Ag-NPs, the chemical environment, and the dielectric medium.[40] Therefore, the UV−vis spectra of the Ag-NPs from *B. nivosa* extract exhibited an absorbance peak in the range of 400−438 nm after the reduction of Ag ions, confirming the presence of silver nanoparticles. The results of the UV−vis spectra are in agreement with the findings reported in the literature, further validating the successful synthesis of Ag-NPs using *B. nivosa* extract.[41]

FT-IR Analysis. FT-IR analysis of the fabricated Ag-NPs was performed to determine the functional groups present on the surface as well as their interactions with the Ag-NPs (Figure 5). The absorption peak at 3298 cm^{-1} represents the stretching vibrations of the −OH group, suggesting the presence of hydroxyl groups on the nanoparticle surface. The peak at 2353 cm^{-1} indicated the presence of carbon dioxide (CO_2). The peak at 2117 cm^{-1} was attributed to the presence of a −C−O bond, revealing the involvement of this bond within the Ag-NPs. The peak at 1685 cm^{-1} indicated the presence of a C=O stretching vibration from a carboxylic acid (−COOH). The 1008 cm^{-1}, peak was attributed to C−O bond stretching from alcohol (−OH), representing functional groups from metab-

olites covering the Ag-NPs. The peak at 800 cm^{-1} suggested the presence of an aromatic ring while the peak at 1507 cm^{-1} was due to aromatic stretching vibrations. The peak at 1990 cm^{-1} indicated the presence of NCO functional group from isocyanates (R−N=C=O). Overall, the FT-IR analysis provided valuable information about the various functional groups present on the surfaces of the fabricated Ag-NPs and the interactions within the Ag-NPs.

X-ray Diffraction Analysis. Figure 6 depicts the XRD patterns of the synthesized Ag-NPs from *B. nivosa* extract. The XRD spectra showed distinct diffraction peaks at 38.6, 46.4, 60.8, and 77.5°, which were attributed to the 111, 200, 220, and 311 reflection Bragg's planes, respectively. These XRD patterns indicated the face-centered cubic structure of the synthesized Ag-NPs, suggesting their crystalline nature. The XRD results are in accordance with the existing literature and well matched with JCPDS No. 04−0783, which is the standard reference for Ag-NPs.[42]

Furthermore, additional peaks were observed alongside the standard peaks of silver, indicating the presence of phytochemicals from *B. nivosa* acting as the capping agent. The coexistence of these additional peaks indicated the interaction of the phytochemicals with the surface of the Ag-NPs. The average size of the crystalline Ag-NPs was assessed utilizing the Debye−Scherer equation. This equation is a valuable tool in determining nanoparticle size by analyzing their XRD patterns. The Debye−Scherer equation relates the crystallite size to the broadening of XRD peaks, offering insights into the dimensions of the nanoparticles. This method provides crucial information about the structural characteristics of Ag-NPs, enhancing our understanding of their size
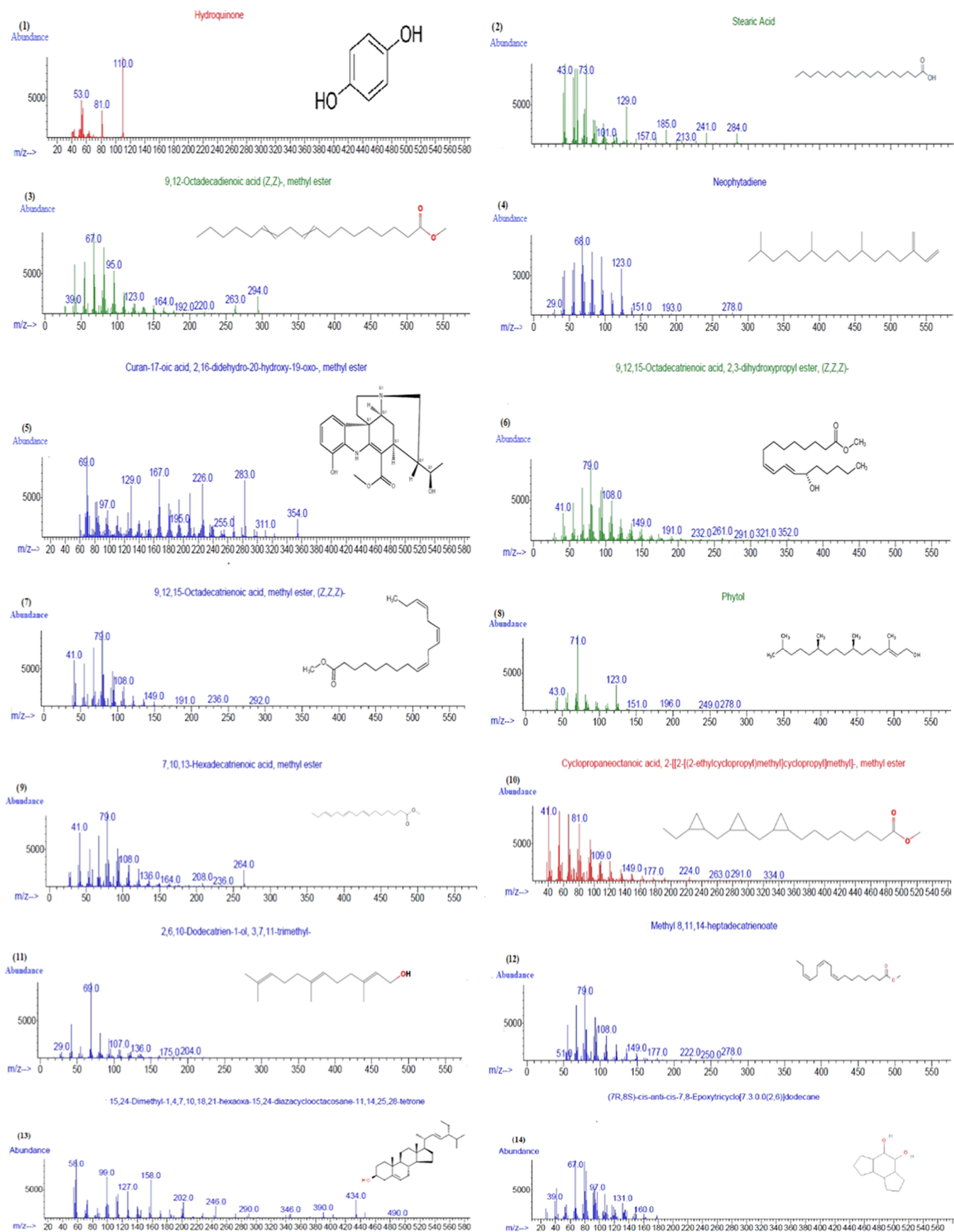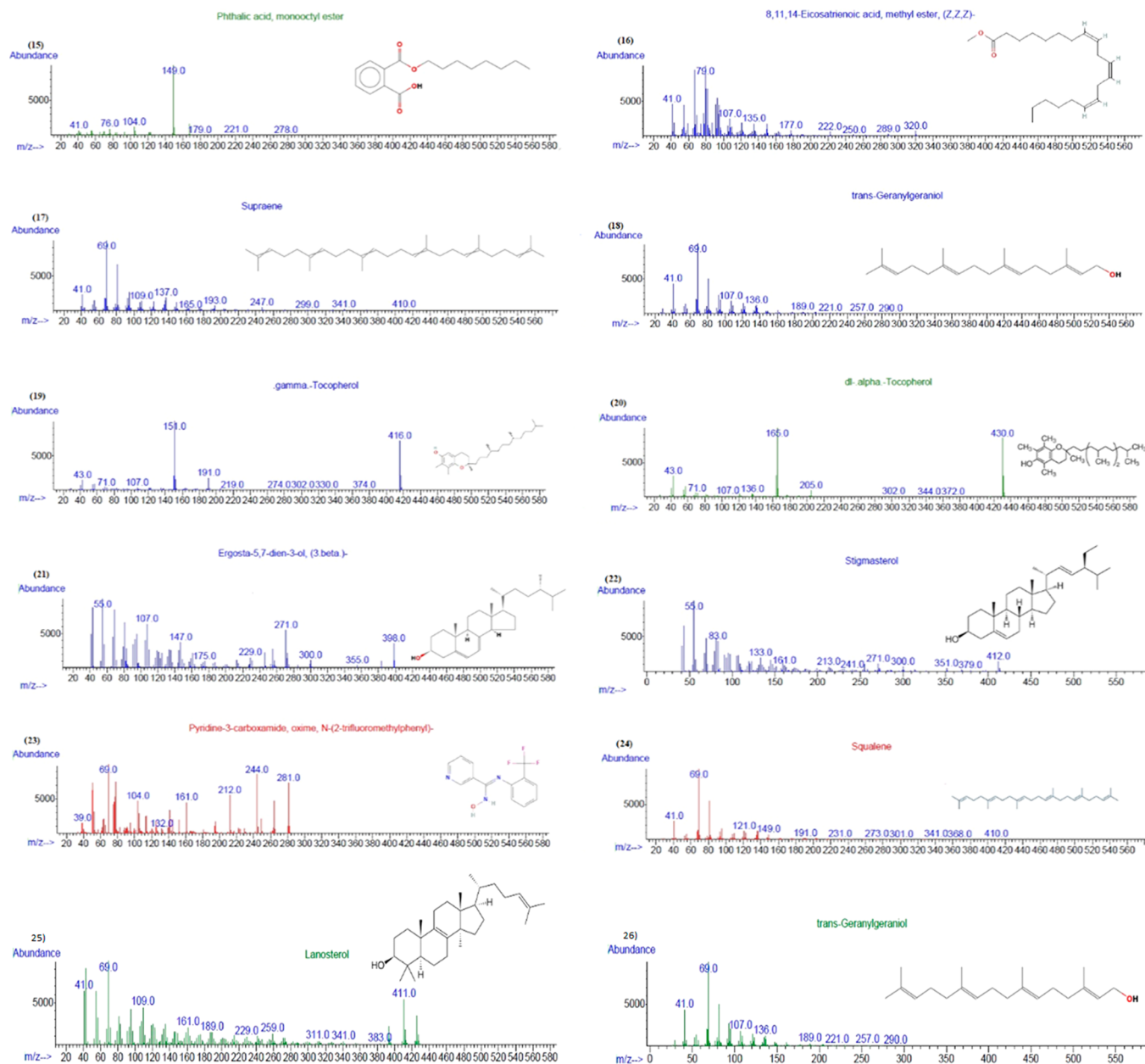
Figure 3. continued

Figure 3. Mass spectra of 26 identified compounds from the *B. nivosa* extract.
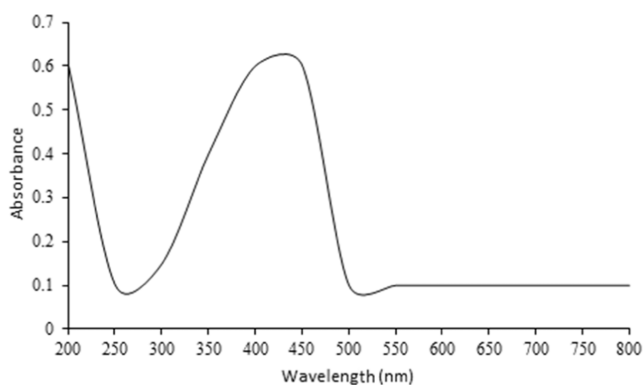

Figure 4. UV−vis spectra of synthesized silver nanoparticles from the methanolic extract of *B. nivosa* extract.

distribution within the sample. This characterization technique confirmed the formation of crystalline Ag-NPs and their structural properties.

$$D = \frac{k\lambda}{\beta \cos \theta} \tag{6}$$

where D represents the average crystalline size of the fabricated Ag-NPs (in nm), k embodies Scherrer's constant with a value of 0.9 (for a spherical shape), λ depicts the wavelength of X-ray (1.54 Å), β shows the full width at half-maximum of the Bragg's angle (2θ) reflection of 111, and θ represents the Bragg angle of diffraction.[43] Using the Debye−Scherer equation and analyzing the XRD pattern, we found the average crystalline size of the fabricated Ag-NPs to be 21.05 nm. From the XRD pattern, it was inferred that the major crystalline phase indicated the presence of Ag-NPs.
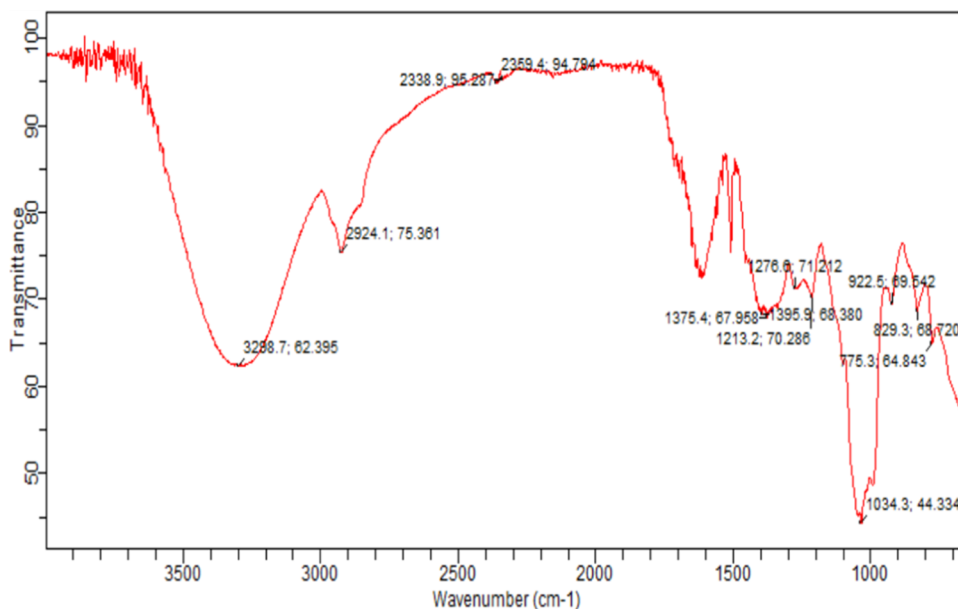
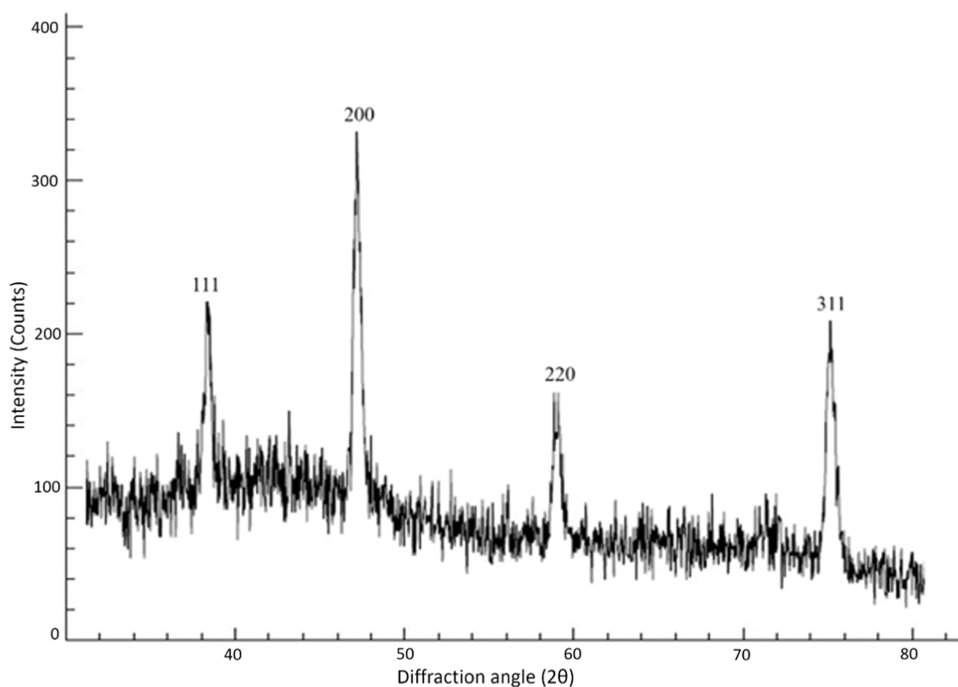**Figure 5.** FT-IR spectrum of synthesized silver nanoparticles from a methanolic extract of *B. nivosa* extract.

Figure 6. XRD spectra of silver nanoparticles *B. nivosa* extract.

Scanning Electron Microscopy. Scanning electron micrographs (at magnifications (a) 1661×, (b) 2220×, and (c) 3261×) of the Ag-NPs synthesized from *B. nivosa* extract are presented in Figure 7. The capping agents from the *B. nivosa* extract were combined with $AgNO_3$ to synthesize the Ag-NPs. SEM analysis was performed to investigate the shape, size, and morphology of the prepared Ag-NPs.

The SEM images revealed small agglomerates of Ag-NPs with irregular surfaces, indicating the attachment of phytochemicals, possibly from the *B. nivosa* extract on the surface of the Ag-NPs. The presence of these phytochemicals contributes to the capping and stabilization of the Ag-NPs. The SEM analysis provides valuable visual information about the surface characteristics and aggregation behavior of the synthesized nanoparticles supporting their potential application in various fields.

Energy-Dispersive X-ray Analysis. EDX analysis was employed to determine the elements and their relative abundances in the biosynthesized Ag-NPs, as illustrated in Figure 8. The EDX graphical representation provided insights into the purity and precise chemical composition of the Ag-NPs. The presence of silver in the synthesized Ag-NPs was notably prominent when compared to other elements, including carbon (C), chlorine (Cl), oxygen (O), and aluminum (Al). The reduced Ag-NPs exhibited a characteristic optical absorption peak at 3 keV, attributed to the phenomenon of surface plasmon resonance (SPR).[44] The EDX spectrum indicated the percentage of the relative
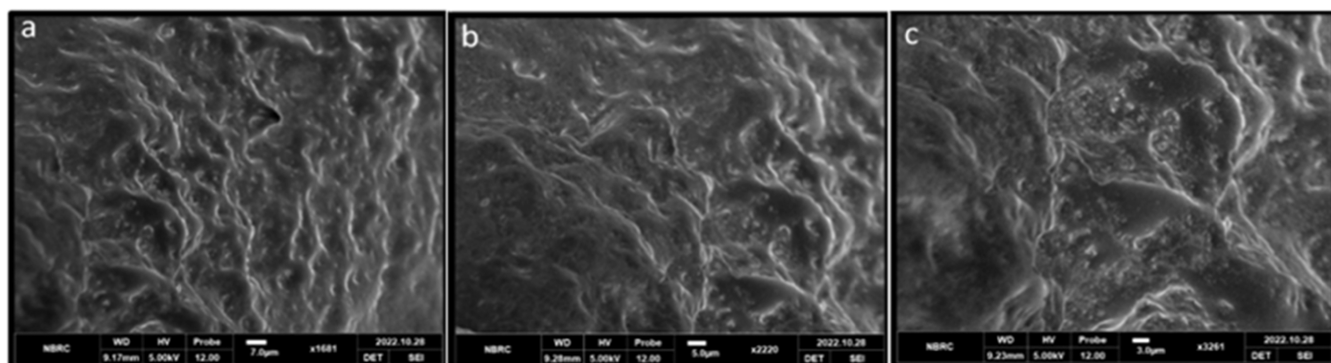
Figure 7. Scanning electron micrograph (SEM) of silver nanoparticles of *B. nivosa* extract at different magnifications: (a) 1661×, (b) 2220×, and (c) 3261×.
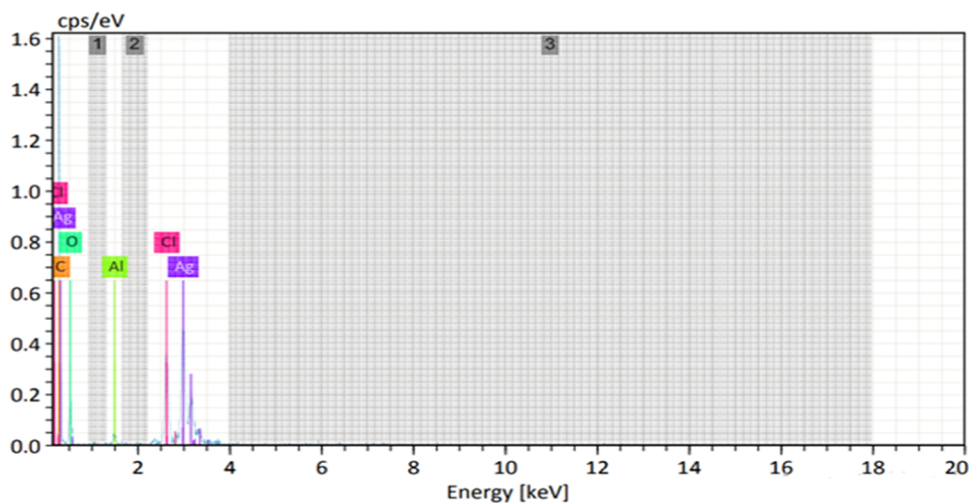

Figure 8. Graphical description of energy-dispersive X-ray (EDX) of synthesized silver nanoparticles from *B. nivosa* extract.
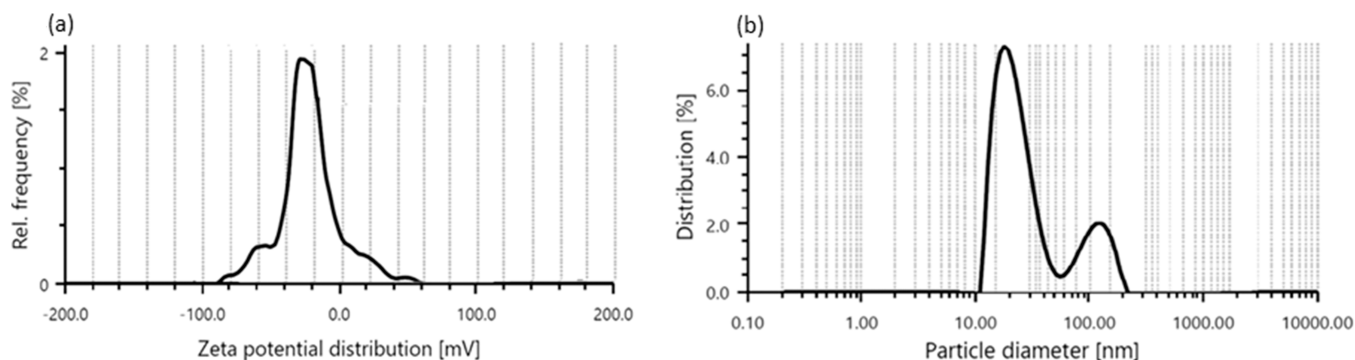

Figure 9. ζ-potential (a) and particle size distribution curve (b) for synthesized silver nanoparticles from *B. nivosa*.

composition of elements with silver at 21.52%, carbon at 54.11%, chlorine at 5.63%, oxygen at 19.68%, and aluminum at 0.63%. The other elements acted as capping agents, binding to the synthesized Ag-NPs.[45]

ζ-Potential Analysis. The measured ζ-potential value of the synthesized Ag-NPs was −31.78 mV, as depicted in Figure 9a, indicating the stability of these Ag-NPs. A higher negative ζ-potential value signifies that the Ag-NPs are stable with no agglomerates present. The negative ζ-potential observed in our study can be attributed to the presence of phytochemical capping agents in the leaf extract of *B. nivosa*. These phytochemicals are likely responsible for forming a protective

layer around the nanoparticles, preventing agglomeration and enhancing their stability.

Dynamic Light Scattering Analysis. DLS is used to characterize the distribution of the size and monodispersing quantity in colloidal solutions. In the present study, DLS analysis was performed to obtain the intensity and number of particles related to the size distribution of the synthesized Ag-NPs from *B. nivosa*. The DLS study demonstrated that the size range of *B. nivosa*-mediated Ag-NPs is from 10 to 295 nm with an average particle size intensity at 25 nm as shown in Figure 9b. This result is in agreement with previous DLS findings reported in the literature.[46] DLS is a powerful technique that
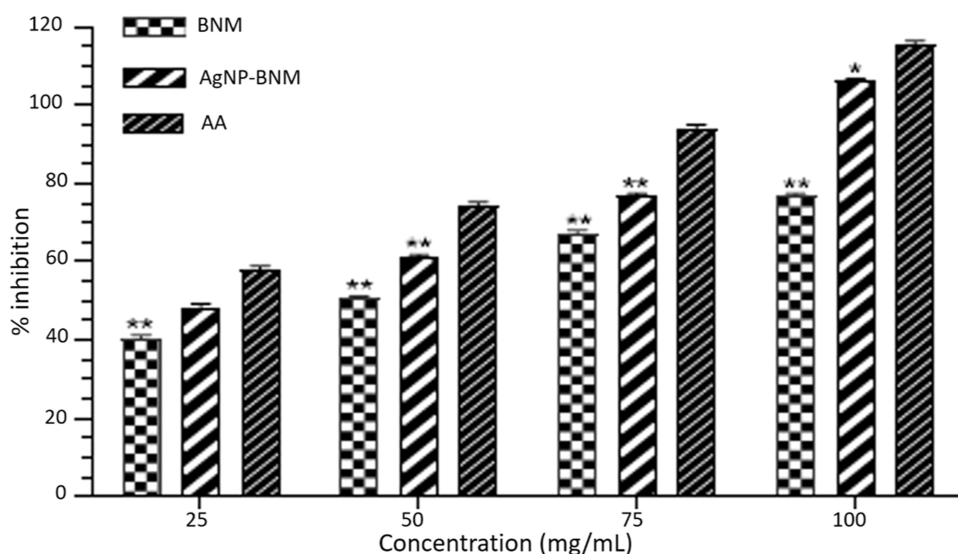
Figure 10. Antioxidant activity of *B. nivosa* extract and Ag-NPs was determined by DPPH free radicals scavenging activity, while ascorbic acid was used as standard. To calculate the statistical results, one-way ANOVA was performed followed by Tukey's multiple comparison test. The results are presented as mean ± standard deviation (SD), while **represents $P < 0.01$, * represents $P < 0.05$, and ns = nonsignificant. Abbreviation: BNM: *B. nivosa* methanolic extract, AgNP-BNM: Silver nanoparticles of methanolic extract of *B. nivosa*, AA: Ascorbic acid.

provides valuable information about the size distribution and stability of Ag-NPs in solution.

***In Vitro* Analysis of Pharmacological Activities.**
Analysis of Antioxidant Activity. The antioxidant activity of both the *B. nivosa* extract and the fabricated Ag-NPs from *B. nivosa* was determined using DPPH at various concentrations (25, 50, 75, and 100 μg/mL). Ascorbic acid was used as the standard antioxidant for comparison.[47] The results indicated that the *B. nivosa* methanolic extract at 100 μg/mL exhibited 75% inhibition of DPPH activity, showing significant antioxidant activity compared to that of the standard (Figure 10). This demonstrates that the phytochemicals present in the *B. nivosa* extract donate hydrogen atoms from the hydroxyl groups to eliminate free radicals.[48] In the case of the fabricated Ag-NPs of *B. nivosa* extract, an even higher DPPH activity of 105% was reported, as shown in Figure 10 and Table 4, indicating significant antioxidant potential compared to that of the standard.

This result indicates that the Ag-NPs have the ability to scavenge free radicals.[49] The presence of phytochemicals containing hydroxyl groups on the surface of Ag-NPs contributes to the stabilization of radicals, further enhancing their free radical scavenging potential. Ag-NPs rapidly react with free radicals.[50] The IC$_{50}$ value, which indicates the total amount of antioxidants required to reduce the initial concentration of DPPH free radicals by 50%, was determined. A low IC$_{50}$ value indicates higher antioxidant activity, and in this study, the synthesized Ag-NPs showed promising antioxidant activity, suggesting their potential use as free radical scavengers in biomedical applications.[51] This result infers that Ag-NPs can be used as free radical scavengers in biomedical practices.

Analysis of Cytotoxic Activity. To assess the anticancer activity of the *B. nivosa* extract and the Ag-NPs prepared from it, an MTT assay was conducted using MCF7 breast cancer cells. This assay involved measuring the dose-dependent response of these substances to determine the concentration at which they inhibited cell growth, known as the inhibitor concentration (IC$_{50}$). The obtained results revealed that both

Table 4. Different Concentrations of *B. nivosa* Methanolic Extract and Silver Nanoparticles Showed 50% DPPH Free Radical Scavenging Activity[a,b]

samples	conc (μg/mL)	% of inhibition	IC$_{50}$ value
BNM	25	41 ± 1.95**	1.51 ± 0.05
	50	52 ± 1.09**	
	75	67 ± 2.04**	
	100	75.9 ± 2.04**	
AgNP-BNM	25	47.54 ± 5.13^{ns}	1.21 ± 0.75
	50	61.98 ± 3.24**	
	75	76.68 ± 4.12**	
	100	105.01 ± 2.26*	
AA	25	56.4 ± 3.13	1.19 ± 0.93
	50	76.8 ± 1.93	
	75	92.23 ± 3.01	
	100	117.23 ± 2.95	

[a]The results are presented as mean ± standard deviation (SD), while **represents $P < 0.01$, * represents $P < 0.05$, and ns = nonsignificant. [b]Abbreviations: BNM: *B. nivosa* methanolic extract, AgNP-BNM: Silver nanoparticles of methanolic extract of *B. nivosa*, AA: Ascorbic acid.

B. nivosa extract and the Ag-NPs exhibited significant potential in inhibiting the proliferation of MCF7 cancer cells, with IC$_{50}$ values of 67 and 55 μg/mL, respectively (Figure 11). These findings are highly promising as they indicate that both the plant extract and the synthesized Ag-NPs possess strong cytotoxic properties against breast cancer cells. The lower IC$_{50}$ values for the silver nanoparticles suggest that they may be more effective in inhibiting the growth of MCF7 cells compared to that of the extract alone. Therefore, the results of the MTT assay underscore the cytotoxic potential of *B. nivosa* in the context of breast cancer and hold promise for potential applications in cancer therapy.

Analysis of Acetylcholinesterase Inhibition Activity. The results demonstrated that both *B. nivosa* extract and Ag-NPs exhibited a significant level of inhibition of acetylcholinesterase activity, as presented in Table 5. Specifically, *B. nivosa* extract
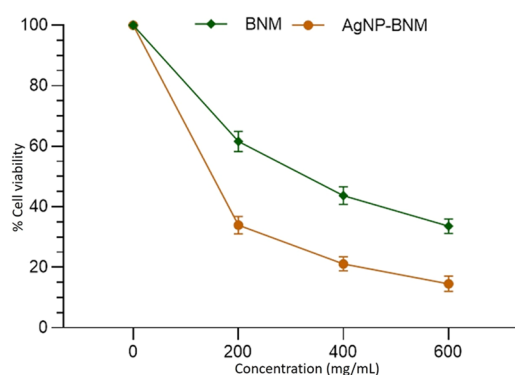
Figure 11. Cytotoxic activity of the *B. nivosa* extract and synthesized nanoparticles. Abbreviations: BNM: Methanolic extract of *B. nivosa*, AgNP-BNM: Silver nanoparticles were synthesized from a methanolic extract of *B. nivosa*.

Table 5. *In Vitro* Inhibitory Activities of *B. nivosa* Extract and Nanoparticles for Acetylcholinesterase and α-Amylase

samples	acetylcholinesterase inhibition		α-amylase inhibition	
	inhibition of acetylcholinesterase	IC$_{50}$ (μM)	inhibition of α-amylase	IC$_{50}$ (μM)
BNM	39.87 ± 0.09	1.15	48.89 ± 0.78	2.25
AgNP-BNM	87.12 ± 0.34	0.09	67.98 ± 0.57	1.51
positive control	eserine 81.89 ± 0.45	0.03	acarbose 79.98 ± 0.92	1.24

and the Ag-NPs displayed inhibitory percentages of 39.87 ± 0.09 and 87.12 ± 0.34, respectively, with corresponding IC$_{50}$ values of 1.15 and 0.09. As a reference, eserine was used, and it exhibited the highest inhibitory activity against acetylcholinesterase, with a percentage inhibition of 81.89 ± 0.45 and an IC$_{50}$ value of 0.03. These findings highlight the considerable potential of both the *B. nivosa* extract and Ag-NPs in inhibiting the activity of acetylcholinesterase. Acetylcholinesterase is an enzyme involved in the breakdown of acetylcholine, a neurotransmitter. Inhibiting this enzyme can have various implications, particularly in the context of neurological and neurodegenerative disorders. The lower IC$_{50}$ values for both the *B. nivosa* extract and the Ag-NPs suggest that they are effective inhibitors of acetylcholinesterase, with Ag-NPs being particularly potent. This research holds promise for potential applications in areas related to neurobiology and therapeutics, where acetylcholinesterase inhibitors play a crucial role.

Analysis of α-Amylase Inhibition Activity. B. nivosa and the synthesized Ag-NPs exhibited *in vitro* inhibitory activity against α-amylase, as presented in Table 5. The *in vitro* inhibitory effect of *B. nivosa* and Ag-NPs on the enzymatic activity of α-amylase was assessed by using starch as the substrate. The results indicated that *B. nivosa* extract and the synthesized Ag-NPs demonstrated a percentage inhibition of 48.89 ± 0.78 and 67.98 ± 0.57, respectively, with IC$_{50}$ values of 2.25 and 1.51. These values were compared to those of acarbose, a known reference compound. The findings signify that both the *B. nivosa* extract and silver nanoparticles possess the ability to inhibit the enzymatic activity of α-amylase, which plays a crucial role in starch digestion. Inhibition of α-amylase can be beneficial in managing conditions like diabetes as it can help reduce postmeal spikes in blood sugar levels. The lower IC$_{50}$ values for Ag-NPs suggest that they are more potent inhibitors of α-amylase activity compared to the *B. nivosa* extract alone.

■ DISCUSSION

Green synthesis of metallic nanoparticles using plant extracts has gained significant attention due to its economical and environmentally friendly nature. The green synthesis method not only avoids the production of toxic materials but also protects the final product from unfavorable contamination. This advantageous feature makes nanoparticles suitable for therapeutic and diagnostic applications.[52] Initially, green synthesis of nanoparticles was primarily performed using selected compounds, particularly phenolic acids, known for their high reduction potential.[53] Nanoparticles synthesized from natural sources have complex compositions of phytochemicals acting as reducing agents and stabilizers to ensure the monodispersity of the synthesized nanoparticles. The presence of various endogenous substances and antioxidants in the sample can contribute to this process, making it nonselective. The literature also highlights the suitability and advantages of different raw materials that can be used for the preparation of nanoparticles through a green synthesis. However, direct comparison between these materials becomes difficult due to variations in the methods and conditions of synthesis.[54] Green synthesis of nanoparticles has become a prominent area of modern nanotechnology. It is currently being extensively explored that the experimental process for the green synthesis of nanoparticles has emerged as an important and promising branch of nanotechnology. The continuous advancements in this field open new possibilities for innovative applications and developments in various industries and research fields.

This study focuses on the green synthesis of Ag-NPs using *B. nivosa* extract and explores *in vitro* pharmacological activities. The preliminary analysis of phytochemicals in the methanolic extract of *B. nivosa* confirmed the presence of alkaloids, flavonoids, glycosides, saponins, and tannins. These phytochemicals are known to contribute to the pharmacological activities of *B. nivosa*. The findings from our study are consistent with the reported results in the existing literature.[38]

The various compounds identified from *Breynia* species were categorized into different groups, including aromatic ketones, flavonoids, alkaloids, lignans, glycosides, catechins, tannins, terpenoids, and steroids.[55] The pharmacological activities of medicinal plants are often rooted in the phytochemical constituents that they contain. This study aimed to elucidate the presence of phytoconstituents through HPLC and GC-MS. A total of 26 bioactive compounds were identified from the methanolic extract of *B. nivosa* using GC-MS. Among these compounds, hydroquinone was found, which is known for its antioxidant and cytoprotective properties.[56] Stearic acid[57] and neophytadiene[58] were identified as compounds with potential neuroprotective effects, operating through mechanisms dependent on the phosphatidylinositol 3-kinase pathway and the GABAergic system, respectively. Another compound, 9,12-octadecadienoic acid (Z,Z)-, methyl ester, exhibited anti-inflammatory, ulcerogenic, and analgesic activities.[59] Methyl 9-*cis*,11-*trans*-octadecadienoate was found to have dienophilic activity.[60] Furthermore, 9,12,15-octadecatrienoic acid, methyl ester, (Z,Z,Z)-, was previously isolated from the extract of Archidium ohioense and has demonstrated antibacterial, antioxidant, antiarthritic, anticancer, and antipyretic activities.[61] Phytol was reported to possess neuroprotective, antimicrobial, anti-inflammatory, antioxidant, and anticancer properties. Phthalic acid, monooctyl ester was noted for its

anti-inflammatory activity.[59] Supraene, identified in *Cucurbita moschata* extract, exhibits anesthetic activity.[62] Lanosterol and stigmasterol, identified through GC-MS analysis of the genus Euphorbia, are associated with antimicrobial activity.[63] Geranylgeraniol was found to play a role in enhancing testosterone production.[64] The metabolomic profile of the *B. nivosa* extract confirms the presence of numerous potential bioactive compounds. We have identified a variety of bioactive compounds from *B. nivosa*, each with distinct pharmacological activities, ranging from antioxidant and anti-inflammatory properties to potential neuroprotective, antimicrobial, anti-cancer, and anesthetic effects. These findings highlight the rich diversity of compounds within *B. nivosa* and suggest their potential in various health-related applications.

When the methanolic extract of *B. nivosa* was added to the solution of AgNO$_3$, a noticeable change in color appeared, confirming the reduction of AgNO$_3$ to Ag-NPs. This color change was attributed to the SPR phenomenon exhibited by Ag-NPs.[65] The intensity of the color change was estimated by the number of free electrons generated during the reduction of nitrate to nitrite (NO$_3$ to NO$_2$) which mainly reduces silver ions in this process.[66] Our results are consistent with previous research reported in the literature, as the observations regarding the change in color of the reaction mixture were found to be identical.[67] The phenomenon of color change during the synthesis of Ag-NPs from plant extracts is well-established, and it serves as a visual indicator of the successful formation of nanoparticles. The presence of SPR and the subsequent color change are important characteristics that confirm the reduction of silver ions to Ag-NPs.

The Ag-NPs were characterized by using a UV−vis spectrophotometer, which is a fundamental technique for analyzing nanoparticles. The UV−vis spectra were obtained in the range of 200−800 nm. The reduction of silver ions in the reaction mixture, facilitated by the ingredients present in the methanolic extract of *B. nivosa*, was also observed through the UV−vis spectra. When the methanolic extract of *B. nivosa* was mixed with an aqueous solution of AgNO$_3$, a change in color from yellow to brown occurred due to the vibrations of the surface plasmon which serves as an indicator for the formation of Ag-NPs.[68] The UV−vis spectrum of the colloidal solution of Ag-NPs was measured as a function of time by using a cuvette with AgNO$_3$ as the standard. The UV−vis spectrum exhibited absorbance at 400−438 nm which is characteristic of SPR and confirmed the presence of Ag-NPs. UV−vis spectroscopy is a powerful tool for characterizing nanoparticles, and the observed SPR peak in the UV−vis spectrum is a signature feature of the presence of Ag-NPs. This confirms the successful green synthesis of Ag-NPs from the *B. nivosa* extract, providing essential information about their optical properties and stability.

In the UV−vis spectrum, the observed peak broadening indicates that the dispersion of the particles is relatively poor. The reduction of silver ions along with the formation and stabilization of Ag-NPs occurred within 120 min of the reaction. This process is noteworthy for its rapidity, making it one of the fastest bioreducing methods for the synthesis of silver nanoparticles.[69] The position of the surface plasmon band in the solution of Ag-NPs remains near 400 nm indicating that there are no significant agglomerations, and the particles are well dispersed in the solution.[70] This is an essential characteristic for the successful synthesis of stable and monodispersed nanoparticles, ensuring their potential applica-

tion in various fields including biomedicine and catalysis. The UV−vis spectrum provides valuable insights into the optical properties and stability of the synthesized Ag-NPs, which are crucial for their practical utilization and further functionalization.

The FT-IR spectra of the fabricated Ag-NPs provided detailed insights into the functional groups present on the nanoparticle surface and their interactions with the nanoparticles. The peaks observed in FT-IR analysis indicated the presence of various functional groups, suggesting that phytochemicals in the methanolic extract of *B. nivosa* acted as capping agents for Ag-NPs. The FT-IR analysis not only identified specific functional groups but also provided evidence of the involvement of phytochemicals in the reduction, capping, and stabilization of the Ag-NPs. The FT-IR analysis identified the specific functional groups and provided evidence of the involvement of phytochemicals in the reduction, capping, and stabilization of the Ag-NPs. These observed peaks collectively pointed toward the diverse functional groups associated with the synthesized Ag-NPs, consistent with previously reported findings.[38,71] The methanolic extract of *B. nivosa* is rich in flavonoids, phenols, saponins, terpenoids, and polyphenolics, which acted as capping agents, preventing the agglomeration and ensuring nanoparticle stability, which is crucial for maintaining the stability and uniformity of the synthesized Ag-NPs making them suitable for various applications. The FT-IR analysis further confirmed the presence of these secondary metabolites in the methanolic extract of *B. nivosa*, which play a significant role in the reduction, capping, and stabilization of Ag-NPs. The bonding abilities of moieties, such as carboxyl, carbonyl, and hydroxyl, in these secondary metabolites played a pivotal role in the formation and stability of Ag-NPs. During the formation of silver nanoparticles, Ag$^+$ ions and free radicals present in the flavonoids form an intermediate complex which then undergoes oxidation leading to the production of the keto form and the reduction of silver (Ag$^+$ to Ag^0), ultimately resulting in the synthesis of Ag-NPs.[72] The FT-IR results strongly support the role of plant-derived phytochemicals in the green synthesis process and highlight their significance in the functionalization of Ag-NPs for various applications.

XRD is a technique used to determine the structure of crystals and the chemical composition of materials. In our experiment, XRD was employed to detect the presence of Ag-NPs by analyzing the diffraction peaks in the XRD spectra. The XRD pattern showed distinct peaks at 38.6, 46.4, 60.8, and 77.5° corresponding to Bragg's reflection planes 111, 200, 220, and 311, respectively. In addition to the Bragg's peaks, unassigned peaks were also observed indicating the presence of phytochemicals on the surface of Ag-NPs.[73] The slight line broadening of all peaks is attributed to the small size of the synthesized Ag-NPs. These results are consistent with previously reported findings.[74] The XRD results further confirmed that the Ag-NPs are formed through the reduction of silver ions by the methanolic extract of *B. nivosa*.[75] The XRD analysis is a powerful tool for characterizing the crystal structure and determining the phase composition of the synthesized Ag-NPs. It provides essential information about the nature of Ag-NPs, helping to understand their physical and chemical properties, which is crucial for potential applications in various fields such as medicine, catalysis, and electronics.

The synthesized Ag-NPs exhibited a predominantly spherical shape. The shape of Ag-NPs is known to significantly

influence their electronic and optical properties.[76] The SEM histogram confirmed the spherical shape of the synthesized Ag-NPs with an average diameter in the range of 21.05 nm. This finding aligns with similar observations reported in the literature.[77] The spherical morphology is desirable for many applications due to its enhanced stability and unique properties, making the synthesized Ag-NPs suitable candidates for various biomedical and technological uses. SEM analysis provides valuable visual evidence of the nanoparticle shape and size complementing other characterization techniques like XRD to gain comprehensive insights into the nanoparticle's morphology and structure.

ζ-potential is a crucial factor governing the interaction between positive and negative charges in a particle dispersion and plays a significant role in explaining the stability of nanoparticles and colloidal dispersion.[78] The ζ-potential value directly influences the stability of nanoparticles; higher absolute values of ζ-potential indicate greater stability.[79] This parameter describes the repulsion between the surface charges of the nanoparticles. In our study, the synthesized Ag-NPs exhibited a negative ζ-potential, signifying a negative charge on the nanoparticles' surface. The higher negative value of ζ-potential suggests strong electrostatic repulsion between the particles, preventing agglomeration.[80] Our results for ζ-potential analysis align with those reported for Ag-NPs synthesized from *Ficus religiosa* extract.[81] This enhanced stability is essential for the potential applications in various fields including drug delivery, catalysis, and environmental remediation. ζ-potential analysis provides critical information about the surface charge of Ag-NPs and their stability in a colloidal dispersion, serving as a valuable tool for assessing the effectiveness of surface coatings and stabilizing agents during nanoparticle synthesis, to optimize the production process for specific applications.

DLS is a technique used for the estimation of the particle size and the distribution profile of nanoparticles in a suspension. In DLS, a monochromatic beam of light is directed at the nanoparticles and the changes in the wavelength of light are related to the size of the nanoparticles.[82] The fluctuations in the movement of nanoparticles are caused by Brownian motion which constantly changes over time.[83] DLS analysis confirmed that the average particle size of the fabricated Ag-NPs was 25 nm. DLS is a noninvasive and powerful tool to determine the hydrodynamic size and polydispersity of nanoparticles in a colloidal solution. It provides valuable information about the stability and homogeneity of nanoparticles and is widely used in nanoparticle characterization studies. The obtained average particle size of 25 nm indicates that the green-synthesized Ag-NPs are nanoscale in dimension, making them suitable for various applications in nanomedicine, catalysis, and other nanotechnology-based fields.

Antioxidant activity of the *B. nivosa* extract and Ag-NPs of the *B. nivosa* extract was confirmed using DPPH assay. The percentage of inhibition and the IC_{50} values indicated the antioxidant activity of both Ag-NPs and the extract. The results suggest that the extract has the potential for reduction of silver ions as electron transfer is the main key and dominant mechanism for the green synthesis of Ag-NPs. The DPPH assay is a widely used method to assess the antioxidant potential of natural extracts and Ag-NPs. It measures the ability of the samples to donate hydrogen atoms and neutralize free radicals, thereby reducing the purple color of the DPPH radical

to yellow. The higher percentage of inhibition and lower IC_{50} value indicate stronger antioxidant activity, which is beneficial for scavenging free radicals and protecting cells from oxidative damage. The green synthesis of Ag-NPs using *B. nivosa* extract not only provides a sustainable and environmentally friendly method for nanoparticle production but also enhances their antioxidant potential, making them valuable for biomedical and therapeutic applications.

This study represents the first report of the cytotoxic potential of the *B. nivosa* extract and the Ag-NPs prepared from it. The findings of this research are consistent with a previously reported paper, which also suggested that both the plant extract and Ag-NPs have the potential for cytotoxicity.[84] Notably, Ag-NPs displayed a greater cytotoxic potential compared to the plant extract. This enhanced potential may be attributed to the synergistic effect of nanosized silver and the phytochemical constituents that adhere to the surface of the nanoparticles. Cytotoxic activity of Ag-NPs could also depend on their size, with smaller nanoparticles having greater mobility and potential cytotoxicity,[85] while larger nanoparticles might exhibit reduced cytotoxicity.[86] Previous research has indicated that antioxidant materials like Ag-NPs can reduce tumor cell volume by neutralizing free radicals and inhibiting the proliferation of cancerous cells.[87]

The presence of certain chemicals with enzyme inhibitory activity plays a significant role in determining various pharmacological targets.[88] For instance, acetylcholinesterase is responsible for hydrolyzing acetylcholine into acetyl CoA and choline. A reduced level of acetylcholinesterase can help protect neurons and improve the condition of Alzheimer's disease patients.[89] Given the development of resistance to antihyperglycemic substances, the production of natural inhibitors with high pharmacological activity and minimal side effects is essential. Antidiabetic drugs should ideally have both hypoglycemic and antioxidant effects with minimal side effects.[90] α-amylase is responsible for breaking glycosidic bonds in starch. Flavonoids present in the plant extract inhibit the activity of α-amylase, preventing the conversion of starch into disaccharides within the body. α-amylase aids glucosidase in the formation of monosaccharides from disaccharides, helping to regulate glucose levels.[91] The results of this study align with those reported in a previous research.[92]

The experimental outcomes of all of the characterization techniques presented in this study demonstrate the significance of the results. The proposed green synthesis mechanism suggests that the reduction of silver ions is mainly responsible for the synthesis of stable Ag-NPs. During this process, silver ions gain electrons from hydroxyl groups ($-OH$) present in flavonoids, which are phytoconstituents of the *B. nivosa* extract, as confirmed by FT-IR analysis. The reported phytochemicals in the *B. nivosa* extract react with $AgNO_3$ to synthesize metallic silver, leading to the formation of Ag-NPs. The capping of these Ag-NPs by secondary metabolites prevents agglomeration and ensures their stability. The fabricated Ag-NPs exhibit a high negative ζ-potential indicating their excellent stability in the colloidal solution. Additionally, these Ag-NPs exhibit high antioxidant activity making them beneficial for various applications in the pharmaceutical sector. The presence of natural antioxidant compounds in the *B. nivosa* extract contributes to the enhanced antioxidant potential of the synthesized Ag-NPs. This study provides valuable insights into the green synthesis approach to produce stable and biologically

active Ag-NPs from *B. nivosa* extract, opening avenues for their potential use in medicine and other fields.

Challenges and Limitations in Scaling Up Synthesis Process for Industrial Applications. As we explore the potential industrial applications of green-synthesized Ag-NPs using the methanolic extract of *B. nivosa*, it is imperative to recognize and address certain challenges and limitations associated with scaling up the synthesis process. Achieving reproducibility on a larger scale necessitates careful control over synthesis parameters, including variations in raw materials, extraction procedures, and environmental conditions, which could impact the quality and uniformity of the nanoparticles. Additionally, concerns about production yield and cost efficiency must be addressed to optimize the process for industrial adoption. Ensuring safety compliance and addressing regulatory standards will be critical as the scale of production increases. Furthermore, maintaining the stability of Ag-NPs during storage and transportation on an industrial scale is a crucial consideration.

Feasibility of Integrating Nanoparticles into Drug Delivery Systems. Beyond addressing challenges, it is essential to study the feasibility of combining synthesized Ag-NPs with drug delivery systems. Comprehensive studies on biocompatibility and pharmacokinetics are mandatory to understand the interaction of nanoparticles with biological systems and to measure their safety and efficacy. Leveraging the exceptional properties of Ag-NPs for targeted drug delivery presents an exciting avenue with a focus on developing functionalized Ag-NPs for selective therapeutic agent delivery. Fine-tuning the release kinetics for controlled drug release and investigating sustained release capabilities are crucial for optimizing therapeutic efficacy. Furthermore, understanding the biodegradability and clearance of Ag-NPs postdrug release is pivotal for assessing their long-term impact on drug delivery applications.

CONCLUSIONS

The present study successfully illustrates the eco-friendly synthesis of stable Ag-NPs using the methanolic extract of *B. nivosa*. Initial analysis of the extract unveiled the presence of a diverse array of phytochemicals, which is crucial for both reducing and capping the Ag-NPs. Various characterization techniques, including UV–vis spectroscopy, FT-IR, XRD, and SEM, were employed, collectively confirming the formation of Ag-NPs and providing insights into their size, structure, and morphology. Additionally, ζ-potential and DLS analyses were conducted, revealing high stability and monodispersion of the synthesized Ag-NPs, which are essential properties for maintaining their integrity and effectiveness. The Ag-NPs exhibited remarkable *in vitro* antioxidant, cytotoxicity, acetylcholinesterase inhibition, and α-amylase inhibition activities, positioning them as promising candidates for diverse biomedical and therapeutic applications such as drug delivery, cancer treatment, and potential use in antidiabetic formulations.

In a broader context, this study contributes significantly to the field of green nanotechnology by utilizing natural plant extracts to synthesize nanoparticles with diverse and noteworthy properties. The findings not only underscore the potential of *B. nivosa*-derived Ag-NPs but also emphasize the broader applicability of plant-based sources in the development of innovative nanomaterials for real-world applications. The environmentally friendly synthesis, comprehensive character-

ization, and promising bioactivities make these Ag-NPs valuable for advancing sustainable and green technologies.

AUTHOR INFORMATION

Corresponding Authors

Muhammad Sajid Hamid Akash − *Department of Pharmaceutical Chemistry, Government College University, Faisalabad 38000, Pakistan;* ● orcid.org/0000-0002-9446-5233; Email: sajidakash@gcuf.edu.pk

Kanwal Rehman − *Department of Pharmacy, The Women University, Multan 60000, Pakistan;* Email: kanwalrehman@wum.edu.pk

Authors

Kanwal Irshad − *Department of Pharmaceutical Chemistry, Government College University, Faisalabad 38000, Pakistan*

Ahmed Nadeem − *Department of Pharmacology and Toxicology, College of Pharmacy, King Saud University, Riyadh 11451, Saudi Arabia*

Asif Shahzad − *Department of Biochemistry and Molecular Biology, Kunming Medical University, Yunnan 650031, China*

Complete contact information is available at:
https://pubs.acs.org/10.1021/acsomega.3c10119

Notes

The authors declare no competing financial interest.

REFERENCES

(1) Pandit, C.; Roy, A.; Ghotekar, S.; Khusro, A.; Islam, M. N.; Emran, T. B.; Lam, S. E.; Khandaker, M. U.; Bradley, D. A. Biological agents for synthesis of nanoparticles and their applications. *J. King Saud Univ., Sci.* **2022**, *34* (3), No. 101869.

(2) Nguyen, D. D.; Lai, J.-Y. Synthesis, bioactive properties, and biomedical applications of intrinsically therapeutic nanoparticles for disease treatment. *Chem. Eng. J.* **2022**, *435*, No. 134970.

(3) Keshari, A. K.; Srivastava, R.; Singh, P.; Yadav, V. B.; Nath, G. Antioxidant and antibacterial activity of silver nanoparticles synthesized by Cestrum nocturnum. *J. Ayurveda Integr. Med.* **2020**, *11* (1), 37–44.

(4) Alharbi, N. S.; Alsubhi, N. S.; Felimban, A. I. Green synthesis of silver nanoparticles using medicinal plants: Characterization and application. *J. Radiat. Res. Appl. Sci.* **2022**, *15* (3), 109–124.

(5) Alhumaydhi, F. A. Green Synthesis of Gold Nanoparticles Using Extract of Pistacia chinensis and Their In Vitro and In Vivo Biological Activities. *J. Nanomater.* **2022**, *2022*, No. 5544475.

(6) (a) Arya, A.; Chundawat, T. S. Metal nanoparticles from algae: A green approach for the synthesis, characterization and their biological activity. *Nanosci. Nanotechnol.-Asia* **2020**, *10* (3), 185–202. (b) Oves, M.; Ahmar Rauf, M.; Aslam, M.; Qari, H. A.; Sonbol, H.; Ahmad, I.; Sarwar Zaman, G.; Saeed, M. Green synthesis of silver nanoparticles by Conocarpus Lancifolius plant extract and their antimicrobial and anticancer activities. *Saudi J. Biol. Sci.* **2022**, *29* (1), 460–471. (c) Javed, I.; Hussain, S. Z.; Ullah, I.; Khan, I.; Ateeq, M.; Shahnaz, G.; Rehman, Hu.; Razi, M. T.; Shah, M. R.; Hussain, I. Synthesis, characterization and evaluation of lecithin-based nanocarriers for the enhanced pharmacological and oral pharmacokinetic profile of amphotericin B. *J. Mater. Chem. B* **2015**, *3* (42), 8359–8365.

(7) Javed, R.; Zia, M.; Naz, S.; Aisida, S. O.; Ain, N.; Ao, Q. Role of capping agents in the application of nanoparticles in biomedicine and

environmental remediation: recent trends and future prospects. *J. Nanobiotechnol.* **2020**, *18*, No. 172.

(8) Hembram, K. C.; Kumar, R.; Kandha, L.; Parhi, P. K.; Kundu, C. N.; Bindhani, B. K. Therapeutic prospective of plant-induced silver nanoparticles: application as antimicrobial and anticancer agent. *Artif. Cells, Nanomed., Biotechnol.* **2018**, *46* (sup3), S38–S51.

(9) Jain, S.; Mehata, M. S. Medicinal Plant Leaf Extract and Pure Flavonoid Mediated Green Synthesis of Silver Nanoparticles and their Enhanced Antibacterial Property. *Sci. Rep.* **2017**, *7* (1), No. 15867.

(10) Zheljazkov, V. D.; Kacaniova, M.; Dincheva, I.; Radoukova, T.; Semerdjieva, I. B.; Astatkie, T.; Schlegel, V. Essential oil composition, antioxidant and antimicrobial activity of the galbuli of six juniper species. *Ind. Crops Prod.* **2018**, *124*, 449–458.

(11) (a) Mahadevan, S.; Vijayakumar, S.; Arulmozhi, P. Green synthesis of silver nano particles from Atalantia monophylla (L) Correa leaf extract, their antimicrobial activity and sensing capability of H(2)O(2). *Microb. Pathog.* **2017**, *113*, 445–450. (b) Singh, H.; Du, J.; Singh, P.; Yi, T. H. Ecofriendly synthesis of silver and gold nanoparticles by Euphrasia officinalis leaf extract and its biomedical applications. *Artif. Cells, Nanomed., Biotechnol.* **2018**, *46* (6), 1163–1170.

(12) Umeokoli, B. O.; Onyegbule, F. A.; Okoye, F. B. C.; Wang, H.; Kalscheuer, R.; Müller, W. E. G.; Hartmann, R.; Liu, Z.; Proksch, P. New amide and dioxopiperazine derivatives from leaves of Breynia nivosa. *Fitoterapia* **2017**, *122*, 16–19.

(13) Ezeigbo, O.; Nwachukwu, I.; Ike-Amadi, C.; Suleiman, J. Evaluation of the phytochemical, proximate and mineral constituents of Breynia nivosa leaf. *Int. J. Biochem. Res. Rev.* **2017**, *20* (2), 1–8.

(14) Onyegbule, F. A.; Ilouno, I. O.; Eze, P. M.; Abba, C. C.; Chigozie, V. U. Evaluation of the analgesic, anti-inflammatory and antimicrobial activities of leaf extracts of Breynia nivosa. *Chem. Sci. Rev. Lett.* **2014**, *3* (12), 1126–1134.

(15) Selamoglu, Z. Polyphenolic Compounds in Human Health with Pharmacological Properties. *J. Tradit. Med. Clin. Naturopathy* **2017**, *06* (4), No. 138.

(16) Amadi, E.; Oyeka, C.; Onyeagba, R.; Ugbogu, O.; Okoli, I. Antimicrobial screening of Breynia nivosus and Ageratum conyzoides against dental caries organisms. *J. Biol. Sci.* **2007**, *7* (2), 354–358.

(17) Newsholme, P.; Cruzat, V. F.; Keane, K. N.; Carlessi, R.; de Bittencourt, P. I., Jr. Molecular mechanisms of ROS production and oxidative stress in diabetes. *Biochem. J.* **2016**, *473* (24), 4527–4550.

(18) Münzel, T.; Camici, G. G.; Maack, C.; Bonetti, N. R.; Fuster, V.; Kovacic, J. C. Impact of Oxidative Stress on the Heart and Vasculature: Part 2 of a 3-Part Series. *J. Am. Coll. Cardiol.* **2017**, *70* (2), 212–229.

(19) Butterfield, D. A.; Halliwell, B. Oxidative stress, dysfunctional glucose metabolism and Alzheimer disease. *Nat. Rev. Neurosci.* **2019**, *20* (3), 148–160.

(20) Zulfiqar, H.; Amjad, M. S.; Mehmood, A.; Mustafa, G.; Binish, Z.; Khan, S.; Arshad, H.; Prоćków, J.; de la Lastra, J. M. P. Antibacterial, Antioxidant, and Phytotoxic Potential of Phytosynthesized Silver Nanoparticles Using Elaeagnus umbellata Fruit Extract. *Molecules* **2022**, *27* (18), No. 5847.

(21) Abdullahi, M. N.; Ilyas, N.; Ibrahim, H. Evaluation of Phytochemical Screening and Analgesic Activity of Aqueous Extract of The Leaves of Microtrichia perotitii Dc (Asteraceae) in Mice using Hotplate Method. *Med. Plant Res.* **2013**, *3* (5), 37–43.

(22) Gul, R.; Jan, S. U.; Faridullah, S.; Sherani, S.; Jahan, N. Preliminary Phytochemical Screening, Quantitative Analysis of Alkaloids, and Antioxidant Activity of Crude Plant Extracts from Ephedra intermedia Indigenous to Balochistan. *Sci. World J.* **2017**, *2017*, No. 5873648.

(23) Iqbal, E.; Salim, K. A.; Lim, L. B. L. Phytochemical screening, total phenolics and antioxidant activities of bark and leaf extracts of Goniothalamus velutinus (Airy Shaw) from Brunei Darussalam. *J. King Saud Univ., Sci.* **2015**, *27* (3), 224–232.

(24) Banso, A.; Adeyemo, S. Phytochemical screening and antimicrobial assessment of Abutilon mauritianum, Bacopa monnifera and Datura stramonium. *Biokemistri* **2006**, *18* (1), 39–44.

(25) Celeghini, R. M. S.; Vilegas, J. H. Y.; Lancas, F. Extraction and quantitative HPLC analysis of coumarin in hydroalcoholic extracts of Mikania glomerata Spreng. ("guaco") leaves. *J. Braz. Chem. Soc.* **2001**, *12*, 706–709.

(26) Pinu, F. R.; Edwards, P. J. B.; Jouanneau, S.; Kilmartin, P. A.; Gardner, R. C.; Villas-Boas, S. G. Sauvignon blanc metabolomics: grape juice metabolites affecting the development of varietal thiols and other aroma compounds in wines. *Metabolomics* **2014**, *10* (4), 556–573.

(27) Mahdi, H.; Parveen, A. Synthesis and Characterization of Gold Nanoparticles (Au-NPs) using aqueous extract of Lemongrass. *Int. J. Nanosci.* **2018**, *21* (1), No. 2250008.

(28) Krithiga, N.; Rajalakshmi, A.; Jayachitra, A. Green Synthesis of Silver Nanoparticles Using Leaf Extracts of Clitoria ternatea and Solanum nigrum and Study of Its Antibacterial Effect against Common Nosocomial Pathogens. *J. Nanosci.* **2015**, *2015*, No. 928204.

(29) Savithramma, N.; Rao, M. L.; Devi, P. S. Evaluation of antibacterial efficacy of biologically synthesized silver nanoparticles using stem barks of Boswellia ovalifoliolata Bal. and Henry and Shorea tumbuggaia Roxb. *J. Biol. Sci.* **2011**, *11* (1), 39–45.

(30) Gowramma, B.; Keerthi, U.; Rafi, M.; Rao, D. M. Biogenic silver nanoparticles production and characterization from native stain of Corynebacterium species and its antimicrobial activity. *3 Biotech* **2015**, *5* (2), 195–201.

(31) Erdogan, O.; Abbak, M.; Demirbolat, G. M.; Birtekocak, F.; Aksel, M.; Pasa, S.; Cevik, O. Green synthesis of silver nanoparticles via Cynara scolymus leaf extracts: The characterization, anticancer potential with photodynamic therapy in MCF7 cells. *PLoS One* **2019**, *14* (6), No. e0216496.

(32) Rahman, M. M.; Islam, M. B.; Biswas, M.; Alam, A. H. M. K. In vitro antioxidant and free radical scavenging activity of different parts of Tabebuia pallida growing in Bangladesh. *BMC Res. Notes* **2015**, *8* (1), No. 621.

(33) Heidari, Z.; Salehzadeh, A.; Shandiz, S. A. S.; Tajdoost, S. Anticancer and anti-oxidant properties of ethanolic leaf extract of Thymus vulgaris and its bio-functionalized silver nanoparticles. *3 Biotech* **2018**, *8* (3), No. 177.

(34) Rasul, A.; Yu, B.; Zhong, L.; Khan, M.; Yang, H.; Ma, T. Cytotoxic effect of evodiamine in SGC-7901 human gastric adenocarcinoma cells via simultaneous induction of apoptosis and autophagy. *Oncol. Rep.* **2012**, *27* (5), 1481–1487.

(35) Khan, M.; Yi, F.; Rasul, A.; Li, T.; Wang, N.; Gao, H.; Gao, R.; Ma, T. Alantolactone induces apoptosis in glioblastoma cells via GSH depletion, ROS generation, and mitochondrial dysfunction. *IUBMB Life* **2012**, *64* (9), 783–794.

(36) Asif, H. M. A.; Kamal, S.; Bibi, I.; AlMasoud, N.; Alomar, T. S.; Iqbal, M. Synthesis characterization and evaluation of novel triazole based analogs as a acetylcholinesterase and α-glucosidase inhibitors. *Arabian J. Chem.* **2023**, *16* (4), No. 104626.

(37) Khalid, M. F.; Rehman, K.; Irshad, K.; Chohan, T. A.; Akash, M. S. H. Biochemical Investigation of Inhibitory Activities of Plant-Derived Bioactive Compounds Against Carbohydrate and Glucagon-Like Peptide-1 Metabolizing Enzymes. *Dose-Response* **2022**, *20*, No. 15593258221093275.

(38) Onyegbule, F.; Ilouno, I.; Ikeh, C.; Umeokoli, B.; Eze, P. Evaluation of phytochemical constituents, analgesic, anti-inflammatory, antimicrobial and antioxidant activities of extracts of Breynia nivosa leaves. *Planta Med.* **2014**, *80* (16), No. LP18.

(39) da Silva, R. T. P.; Petri, M. V.; Valencia, E. Y.; Camargo, P. H. C.; de Torresi, S. I. C.; Spira, B. Visible light plasmon excitation of silver nanoparticles against antibiotic-resistant Pseudomonas aeruginosa. *Photodiagn. Photodyn. Ther.* **2020**, *31*, No. 101908.

(40) Link, S.; El-Sayed, M. A. Optical properties and ultrafast dynamics of metallic nanocrystals. *Annu. Rev. Phys. Chem.* **2003**, *54*, 331–366.

(41) Kasthuri, J.; Kathiravan, K.; Rajendiran, N. Phyllanthin-assisted biosynthesis of silver and gold nanoparticles: a novel biological approach. *J. Nanopart. Res.* **2009**, *11* (5), 1075–1085.

(42) Marimuthu, S.; Rahuman, A. A.; Santhoshkumar, T.; Jayaseelan, C.; Kirthi, A. V.; Bagavan, A.; Kamaraj, C.; Elango, G.; Zahir, A. A.; Rajakumar, G.; Velayutham, K. Lousicidal activity of synthesized silver nanoparticles using Lawsonia inermis leaf aqueous extract against Pediculus humanus capitis and Bovicola ovis. *Parasitol. Res.* 2012, *111* (5), 2023–2033.

(43) Kamyar, S.; Ahmad, M.; Zamanian, A.; Sangpour, P.; Shabanzadeh, P.; Abdollahi, Y.; Zargar, M. Green biosynthesis of silver nanoparticles using Curcuma longa tuber powder. *Int. J. Nanomed.* 2012, *7*, 5603–5610.

(44) Kaviya, S.; Santhanalakshmi, J.; Viswanathan, B.; Muthumary, J.; Srinivasan, K. Biosynthesis of silver nanoparticles using citrus sinensis peel extract and its antibacterial activity. *Spectrochim. Acta, Part A* 2011, *79* (3), 594–598.

(45) Dada, A. O.; Adekola, F. A.; Odebunmi, E. O. A novel zerovalent manganese for removal of copper ions: synthesis, characterization and adsorption studies. *Appl. Water Sci.* 2017, *7* (3), 1409–1427.

(46) Das, S. K.; Behera, S.; Patra, J. K.; Thatoi, H. Green Synthesis of Sliver Nanoparticles Using Avicennia officinalis and Xylocarpus granatum Extracts and In vitro Evaluation of Antioxidant, Antidiabetic and Anti-inflammatory Activities. *J. Cluster Sci.* 2019, *30*, 1103–1113.

(47) Salari, S.; Bahabadi, S. E.; Samzadeh-Kermani, A.; Yosefzaei, F. In-vitro Evaluation of Antioxidant and Antibacterial Potential of GreenSynthesized Silver Nanoparticles Using Prosopis farcta Fruit Extract. *Iran. J. Pharm. Res.: IJPR* 2019, *18* (1), 430–455.

(48) Sowndhararajan, K.; Kang, S. C. Free radical scavenging activity from different extracts of leaves of Bauhinia vahlii Wight & Arn. *Saudi J. Biol. Sci.* 2013, *20* (4), 319–325.

(49) Maheshwaran, G.; Bharathi, A. N.; Selvi, M. M.; Kumar, M. K.; Kumar, R. M.; Sudhahar, S. Green synthesis of Silver oxide nanoparticles using Zephyranthes Rosea flower extract and evaluation of biological activities. *J. Environ. Chem. Eng.* 2020, *8* (5), No. 104137.

(50) Vorobyova, V.; Vasyliev, G.; Skiba, M. Eco-friendly "green" synthesis of silver nanoparticles with the black currant pomace extract and its antibacterial, electrochemical, and antioxidant activity. *Appl. Nanosci.* 2020, *10*, 4523–4534.

(51) Medic-Pap, S.; Prvulovic, D.; Takač, A.; Vlajić, S.; Danojević, D.; Takač, A.; Masirevic, S. Influence of tomato genotype to phenolic compounds content and antioxidant activity as reaction to early blight. *Genetika* 2015, *47*, 1099–1110.

(52) (a) Zuorro, A.; Iannone, A.; Natali, S.; Lavecchia, R. Green Synthesis of Silver Nanoparticles Using Bilberry and Red Currant Waste Extracts. *Processes* 2019, *7*, No. 193. (b) Bastos-Arrieta, J.; Florido, A.; Pérez-Ràfols, C.; Serrano, N.; Fiol, N.; Poch, J.; Villaescusa, I. Green Synthesis of Ag Nanoparticles Using Grape Stalk Waste Extract for the Modification of Screen-Printed Electrodes. *Nanomaterials* 2018, *8* (11), No. 946.

(53) Amini, S. M.; Akbari, A. Metal nanoparticles synthesis through natural phenolic acids. *IET Nanobiotechnol.* 2019, *13* (8), 771–777.

(54) Flieger, J.; Flieger, W.; Baj, J.; Maciejewski, R. Antioxidants: Classification, Natural Sources, Activity/Capacity Measurements, and Usefulness for the Synthesis of Nanoparticles. *Materials* 2021, *14* (15), No. 4135.

(55) Saadullah, M.; Asif, M.; Arif, S.; Kanwal, B. A Comprehensive Review on Traditional Uses, Chemical Constituents, and Diverse Pharmacological Importance of the Genus Breynia. *Rec. Nat. Prod.* 2022, *6*, 538–549.

(56) Divya, O.; Pushpakumari, B.; Kumar, D. A.; Nihafiaz, S.; Sameer, P. Evaluation of cytoprotective and in-vivo anti-oxidant activity of Argyreia nervosa leaves extract against hydroquinone induced genotoxicity. *J. Clin. Toxicol.* 2021, *11* (20), No. 1000003.

(57) Wang, Z. J.; Li, G. M.; Nie, B. M.; Lu, Y.; Yin, M. Neuroprotective effect of the stearic acid against oxidative stress via phosphatidylinositol 3-kinase pathway. *Chem.-Biol. Interact.* 2006, *160* (1), 80–87.

(58) Gonzalez-Rivera, M. L.; Barragan-Galvez, J. C.; Gasca-Martínez, D.; Hidalgo-Figueroa, S.; Isiordia-Espinoza, M.; Alonso-Castro, A. J. In Vivo Neuropharmacological Effects of Neophytadiene. *Molecules* 2023, *28* (8), No. 3457.

(59) Mohammed, Y. H.; Mohammad, G.; Hameed, I. Analysis of bioactive chemical compounds of Nigella sativa using gas chromatography-mass spectrometry. *J. Pharmacogn. Phytother.* 2016, *8*, 8–24.

(60) Hashimoto, T.; Suzuki, O.; Tanabe, K. Studies on the thermal polymerization of methyl linoleate. III kinetic approach to the mechanism of thermal dimerization of methyl 9-cis, 11-trans-Octadecadienoate. *J. Jpn. Oil Chem. Soc.* 1968, *17* (10), 550–554.

(61) Godwin, A.; Akinpelu, B.; Makinde, A.; Aderogba, M.; Oyedapo, O. Identification of n-hexane fraction constituents of Archidium ohioense (Schimp. Ex Mull) extract using GC-MS technique. *Br. J. Pharm. Res.* 2015, *6* (6), 366–375.

(62) Muzahid, A. A.; Sharmin, S.; Hossain, M. S.; Ahamed, K. U.; Ahmed, N.; Yeasmin, M. S.; Ahmed, N. U.; Saha, B. K.; Rana, G. M. M.; Maitra, B.; Bhuiyan, M. N. H. Analysis of bioactive compounds present in different crude extracts of Benincasa hispida and Cucurbita moschata seeds by gas chromatography-mass spectrometry. *Heliyon* 2023, *9* (1), No. e12702.

(63) Lehbili, M.; Magid, A. A.; Kabouche, A.; Voutquenne-Nazabadioko, L.; Abedini, A.; Morjani, H.; Gangloff, S. C.; Kabouche, Z. Antibacterial, antioxidant and cytotoxic activities of triterpenes and flavonoids from the aerial parts of Salvia barrelieri Etl. *Nat. Prod. Res.* 2018, *32* (22), 2683–2691.

(64) Ho, H.-J.; Shirakawa, H.; Giriwono, P. E.; Ito, A.; Komai, M. A novel function of geranylgeraniol in regulating testosterone production. *Biosci., Biotechnol., Biochem.* 2018, *82* (6), 956–962.

(65) (a) Salem, S. S.; El-Belely, E. F.; Niedbała, G.; Alnoman, M. M.; Hassan, S. E.-D.; Eid, A. M.; Shaheen, T. I.; Elkelish, A.; Fouda, A. Bactericidal and In-Vitro Cytotoxic Efficacy of Silver Nanoparticles (Ag-NPs) Fabricated by Endophytic Actinomycetes and Their Use as Coating for the Textile Fabrics. *Nanomaterials* 2020, *10* (10), No. 2082. (b) Vanaja, M.; Gnanajobitha, G.; Paulkumar, K.; Rajeshkumar, S.; Malarkodi, C.; Annadurai, G. Phytosynthesis of silver nanoparticles by Cissus quadrangularis: influence of physicochemical factors. *J. Nanostruct. Chem.* 2013, *3* (1), No. 17.

(66) Kang, J. H.; Chae, J. B.; Kim, C. A multi-functional chemosensor for highly selective ratiometric fluorescent detection of silver(I) ion and dual turn-on fluorescent and colorimetric detection of sulfide. *R. Soc. Open Sci.* 2018, *5* (6), No. 180293.

(67) Elumalai, K.; Velmurugan, S. Green synthesis, characterization and antimicrobial activities of zinc oxide nanoparticles from the leaf extract of Azadirachta indica (L.). *Appl. Surf. Sci.* 2015, *345*, 329–336.

(68) Shankar, S. S.; Rai, A.; Ankamwar, B.; Singh, A.; Ahmad, A.; Sastry, M. Biological synthesis of triangular gold nanoprisms. *Nat. Mater.* 2004, *3* (7), 482–488.

(69) Kim, J. S.; Kuk, E.; Yu, K. N.; Kim, J.-H.; Park, S. J.; Lee, H. J.; Kim, S. H.; Park, Y. K.; Park, Y. H.; Hwang, C.-Y.; et al. Antimicrobial effects of silver nanoparticles. *Nanomedicine* 2007, *3* (1), 95–101.

(70) Ankanna, S. T.; Prasad, T. N.; Elumalai, E. K.; Savithramma, N. Production of biogenic silver nanoparticles using Boswellia ovalifoliolata stem bark. *Dig J. Nanomater. Biostruct.* 2010, *5* (2), 369–372.

(71) Alharbi, N. S.; Alsubhi, N. S. Green synthesis and anticancer activity of silver nanoparticles prepared using fruit extract of Azadirachta indica. *J. Radiat. Res. Appl. Sci.* 2022, *15* (3), 335–345.

(72) Joseph, S.; Mathew, B. Microwave-assisted green synthesis of silver nanoparticles and the study on catalytic activity in the degradation of dyes. *J. Mol. Liq.* 2015, *204*, 850–856.

(73) Sathyavathi, R.; Krishna, M. B.; Rao, S. V.; Saritha, R.; Rao, D. N. Biosynthesis of silver nanoparticles using Coriandrum sativum leaf extract and their application in nonlinear optics. *Adv. Sci. Lett.* 2010, *3* (2), 138–143.

(74) Tahir, M. Y.; Ahmad, A.; Alothman, A. A.; Mushab, M. S. S.; Ali, S. Green Synthesis of Silver Nanoparticles Using Thespesia populnea Bark Extract for Efficient Removal of Methylene Blue (MB) Degradation via Photocatalysis with Antimicrobial Activity and for Anticancer Activity. *Bioinorg. Chem. Appl.* 2022, *2022*, No. 7268273.

(75) (a) Udayasoorian, C.; Kumar, K.; Jayabalakrishnan, R. M. Extracellular synthesis of silver nanoparticles using leaf extract of Cassia auriculata. *Dig J. Nanomater. Biostruct.* **2011**, *6* (1), 279−283. (b) Huang, J.; Li, Q.; Sun, D.; Lu, Y.; Su, Y.; Yang, X.; Wang, H.; Wang, Y.; Shao, W.; He, N.; Hong, J.; Chen, C. Biosynthesis of silver and gold nanoparticles by novel sundried Cinnamomum camphora leaf. *Nanotechnology* **2007**, *18*, No. 105104.

(76) Xu, H.; Käll, M. Surface-plasmon-enhanced optical forces in silver nanoaggregates. *Phys. Rev. Lett.* **2002**, *89* (24), No. 246802.

(77) (a) Udayasoorian, C.; Kumar, K. V.; Jayabalakrishnan, M. Extracellular synthesis of silver nanoparticles using leaf extract of Cassia auriculata. *Dig J. Nanomater. Biostruct.* **2011**, *6* (1), 279−283. (b) Chandran, S. P.; Chaudhary, M.; Pasricha, R.; Ahmad, A.; Sastry, M. Synthesis of gold nanotriangles and silver nanoparticles using Aloe vera plant extract. *Biotechnol. Prog.* **2006**, *22* (2), 577−583.

(78) Huynh, N. T.; Passirani, C.; Saulnier, P.; Benoît, J.-P. Lipid nanocapsules: a new platform for nanomedicine. *Int. J. Pharm.* **2009**, *379* (2), 201−209.

(79) Jabr-Milane, L. S.; van Vlerken, L. E.; Yadav, S.; Amiji, M. M. Multi-functional nanocarriers to overcome tumor drug resistance. *Cancer Treat. Rev.* **2008**, *34* (7), 592−602.

(80) Liaqat, N.; Jahan, N.; Anwar, T.; Qureshi, H. Green synthesized silver nanoparticles: Optimization, characterization, antimicrobial activity, and cytotoxicity study by hemolysis assay. *Front. Chem.* **2022**, *10*, No. 952006.

(81) Antony, J. J.; Sithika, M. A.; Joseph, T. A.; Suriyakalaa, U.; Sankarganesh, A.; Siva, D.; Kalaiselvi, S.; Achiraman, S. In vivo antitumor activity of biosynthesized silver nanoparticles using Ficus religiosa as a nanofactory in DAL induced mice model. *Colloids Surf., B* **2013**, *108*, 185−190.

(82) Meva, F. E.; Ntoumba, A. A.; Kedi, P. B. E.; Tchoumbi, E.; Schmitz, A.; Schmolke, L.; Klopotowski, M.; Moll, B.; Kökcam-Demir, Ü.; Mpondo, E. A.; Lehman, L. G. Silver and palladium nanoparticles produced using a plant extract as reducing agent, stabilized with an ionic liquid: sizing by X-ray powder diffraction and dynamic light scattering. *J. Mater. Res. Technol.* **2019**, *8* (2), 1991−2000.

(83) Uma, B.; Swaminathan, T. N.; Radhakrishnan, R.; Eckmann, D. M.; Ayyaswamy, P. S. Nanoparticle Brownian motion and hydrodynamic interactions in the presence of flow fields. *Phys. Fluids* **2011**, *23* (7), No. 73602.

(84) Jeyaraj, M.; Sathishkumar, G.; Sivanandhan, G.; MubarakAli, D.; Rajesh, M.; Arun, R.; Kapildev, G.; Manickavasagam, M.; Thajuddin, N.; Premkumar, K.; Ganapathi, A. Biogenic silver nanoparticles for cancer treatment: an experimental report. *Colloids Surf., B* **2013**, *106*, 86−92.

(85) Park, M. V.; Neigh, A. M.; Vermeulen, J. P.; de la Fonteyne, L. J.; Verharen, H. W.; Briedé, J. J.; van Loveren, H.; de Jong, W. H. The effect of particle size on the cytotoxicity, inflammation, developmental toxicity and genotoxicity of silver nanoparticles. *Biomaterials* **2011**, *32* (36), 9810−9817.

(86) Suman, T. Y.; Rajasree, S. R. R.; Kanchana, A.; Elizabeth, S. B. Biosynthesis, characterization and cytotoxic effect of plant mediated silver nanoparticles using Morinda citrifolia root extract. *Colloids Surf., B* **2013**, *106*, 74−78.

(87) (a) Sangami, S.; Manu, B. Synthesis of Green Iron Nanoparticles using Laterite and their application as a Fenton-like catalyst for the degradation of herbicide Ametryn in water. *Environ. Technol. Innovation* **2017**, *8*, 150−163. (b) Radini, I. A.; Hasan, N.; Malik, M. A.; Khan, Z. Biosynthesis of iron nanoparticles using Trigonella foenum-graecum seed extract for photocatalytic methyl orange dye degradation and antibacterial applications. *J. Photochem. Photobiol., B* **2018**, *183*, 154−163.

(88) Chaudhury, A.; Duvoor, C.; Dendi, V. S. R.; Kraleti, S.; Chada, A.; Ravilla, R.; Marco, A.; Shekhawat, N. S.; Montales, M. T.; Kuriakose, K.; Sasapu, A.; Beebe, A.; Patil, N.; Musham, C. K.; Lohani, G. P.; Mirza, W. Clinical Review of Antidiabetic Drugs: Implications for Type 2 Diabetes Mellitus Management. *Front. Endocrinol.* **2017**, *8*, No. 224539.

(89) Mehta, M.; Adem, A.; Sabbagh, M. New acetylcholinesterase inhibitors for Alzheimer's disease. *Int. J. Alzheimer's Dis.* **2012**, *2012*, No. 728983.

(90) Yang, L. X.; Liu, T. H.; Huang, Z. T.; Li, J. E.; Wu, L. L. Research progress on the mechanism of single-Chinese medicinal herbs in treating diabetes mellitus. *Chin. J. Integr. Med.* **2011**, *17* (3), 235−240.

(91) Elya, B.; Handayani, R.; Sauriasari, R.; Azizahwati; Hasyyati, U. S.; Hasyyati, U. S.; Permana, I. T.; Permana, I. T.; Permatasari, Y. I. Antidiabetic activity and phytochemical screening of extracts from indonesian plants by inhibition of alpha amylase, alpha glucosidase and dipeptidyl peptidase IV. *Pak. J. Biol. Sci.* **2015**, *18* (6), 273−278.

(92) Murugan, R.; Prabu, J.; Chandran, R.; Sajeesh, T.; Iniyavan, M.; Parimelazhagan, T. Nutritional composition, in vitro antioxidant and anti-diabetic potentials of Breynia retusa (Dennst.) Alston. *Food Sci. Hum. Wellness* **2016**, *5* (1), 30−38.